AD-A060 280 NAVY UNDERWATER SOUND LAB NEW LONDON CONN F/G 17/1
A PRELIMINARY COMPARISON OF THE ACOUSTICAL PROPERTIES OF THE B.--ETC(U)
JUL 65 J B DONALD

UNCLASSIFIED USL-TM-932-622-66 NL

1 OF 1
AD A060280

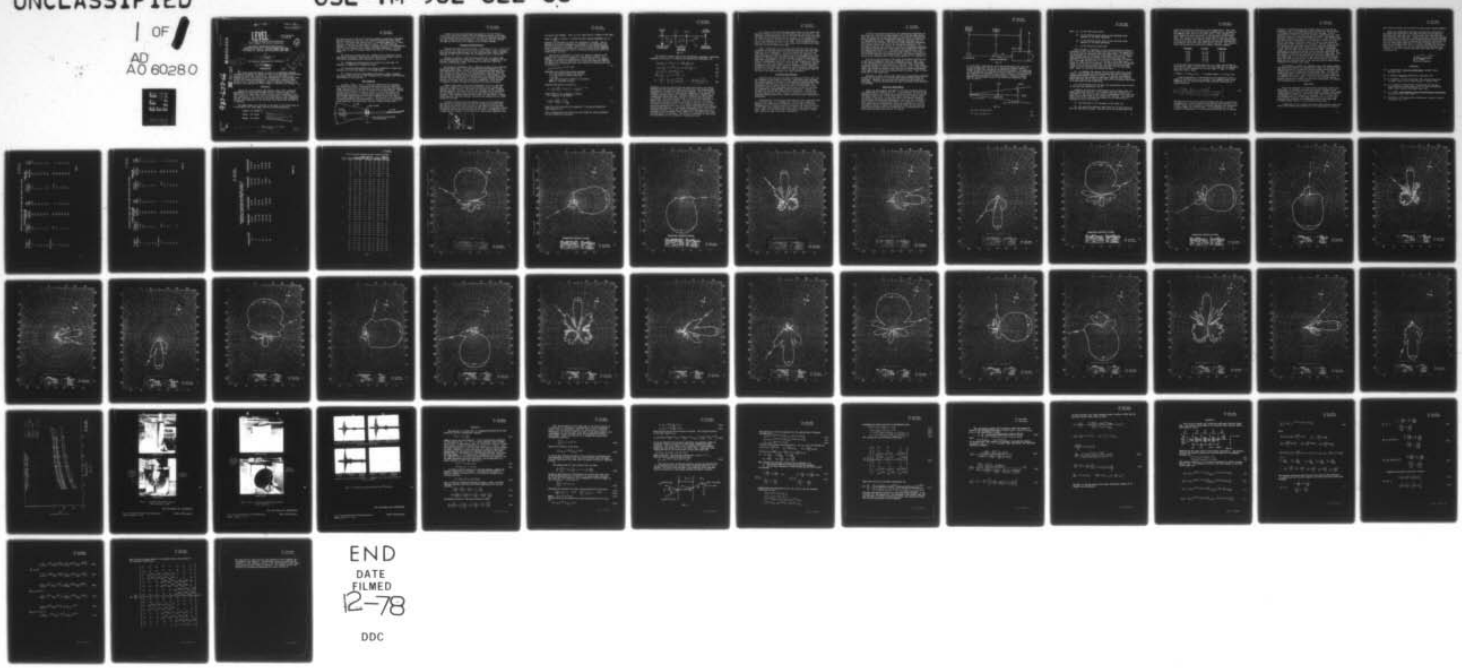

END
DATE FILMED
12-78
DDC

MOST Project-4

Copy to 2

Copy No. MASWSPO

(9) Technical memo.,

LEVEL

USL Problem No. 1-510-00-00

(1) NW

(6)

U. S. Navy Underwater Sound Laboratory
Fort Trumbull, New London, Connecticut

A PRELIMINARY COMPARISON OF THE ACOUSTICAL PROPERTIES OF THE B. F. GOODRICH RUBBER DOME PANEL WITH THOSE OF A 100 MIL. STAINLESS STEEL DOME PANEL.

by

(10) J. B. Donald

USL Technical Memorandum No. 932-622-66

(11) 19 July 1965

(12) 57 p.

DDC
OCT 23 1978
F

AD A060280

002154

DDC FILE COPY

932-622-66

INTRODUCTION

The tests, described herein, are part of a preliminary material investigation program, the object of which is the improvement of materials selected for sonar dome construction. The particular phase of the program covered in this report is the determination of the acoustic properties of a promising dome material, a three-layer laminated rubber product of B. F. Goodrich Company. General background information relating to this dome material may be found in references (a) through (f).

BACKGROUND

During the period 20 March 1965 through 2 April 1965, acoustical measurements were performed at Dodge Pond on a stainless steel dome section and on a rubber dome section of equal overall dimensions. The basic objectives of the tests were the determination of the transmission loss and reflection coefficient of the rubber dome and their comparison with the same properties of the stainless steel dome, which was used as a reference.

The sample domes were contoured to the shape of the forward part of a CW-553/SQS-4 100" sonar dome, with the following dimensions:

Length - 40 inches

Width - 36 inches

Height - 40 inches

(14) USL-TM-932-622-66

This document has been approved for public release and sale; its distribution is unlimited.

002154

Encl (1) to USN/USL ltr ser 932-623 Oct 1966

254 200

The stainless steel dome was of identical material properties as Standard Navy sonar domes, but was only 1/16" thick and lacked the usual inside bracing. The rubber dome supplied by B. F. Goodrich Company was 1" thick and was a lamination of three distinct layers: the first layer was composed of .29 inch neoprene rubber; the second a series of closely-spaced, thin (.12 inch diameter) steel cables sandwiched throughout a .56 inch thick layer (8 ply) of neoprene rubber; the third of .15 inch neoprene rubber.

The domes were mounted with the transmitting (or receiving, as the case may be) projector located within the dome area (see Figs. 1 and 2). Three basic measurements were performed in these tests:

(1) Transmitting beam patterns were plotted for each dome, for purposes of comparison of transmitting loss.

(2) Receiving beam patterns were plotted, primarily to check reciprocity and to note any changes in the formed beams.

(3) Pulsed reflection measurements were made in order to measure the energy reflected from the dome surfaces and to determine the reflection coefficients of the materials.

Test Apparatus

As shown in Figs. 1 and 2, a conically-baffled XU-1347 transducer was used as the acoustic transmitting and receiving device within the dome. The conical unit was mounted at the rear of the dome; the aperture of the projector was on the axis of rotation of the dome fixture. Remote control of the XU-1347 transducer position in the conical baffle was accomplished by means of a flexible cable containing a calibrated rod. This allowed positioning of the XU-1347 Transducer within the dome to obtain peak response (see Fig. 3, below). The position of the transducer for peak response was first determined for each of the test frequencies; these positions, once determined, were held constant during tests.

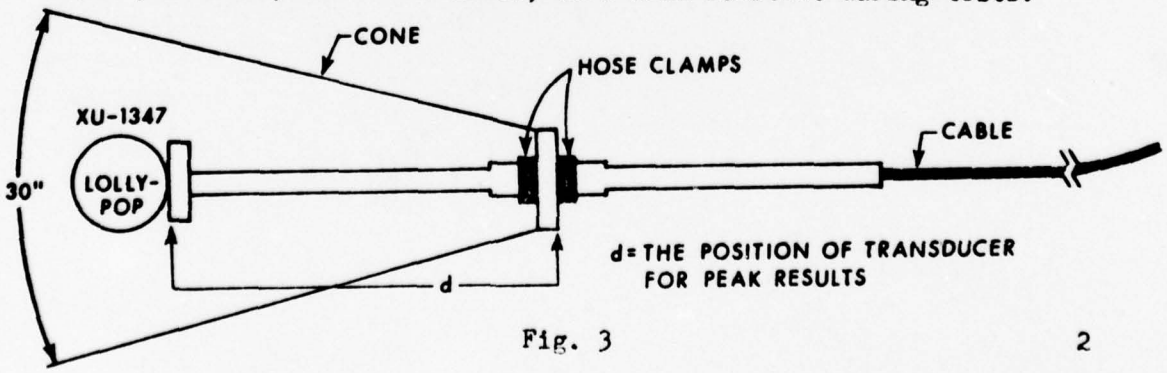

Fig. 3

A Massa 420 Receiving Hydrophone was placed in the far field to receive the transmitted signals from the transducer mounted in the dome. A J-9 transducer was also placed in the far field for transmitting toward the dome in making receiving patterns. Patterns were made by rotating the dome and the conical unit together as an integral package.

Transmitting Beam Patterns

Transmitting beam patterns were made at frequencies of 3.5, 5, 8, 10, 12 and 14 KC, for the stainless steel and the rubber domes. Figs. 4 through 9 show the horizontal beam patterns for the stainless steel dome at relative bearings of 000°, 090°, and 180°, and at frequencies of 3.5 and 14 KC.

Figures 10 through 15 show the beam patterns for the rubber dome for the same bearings and frequencies. Table I gives a comparison of the relative transmission losses, beam widths, and side lobe levels for 3.5, 5, 8, 10, 12, and 14 KC.

By "relative transmission loss", reference is made to the difference in the peak amplitudes of the 000° and 090° patterns compared to the 180° beam pattern, where at 000° and 090° beam patterns were made "looking" through the dome, and at 180° the beam pattern was made "looking" out the open rear (essentially, the same as with no dome present). The major difference between the 000° and the 090° beam patterns arises from the fact that the 000° pattern is obtained "looking" through the front section of the dome (where the curvature is greatest), while the 090° is obtained "looking" through the relatively flat side of the dome.

Table I shows that at the lower frequencies, of 3.5, 5, and 8 KC, there was a negative transmission loss (actually a gain) through the dome for the 000° bearing. One reason for this gain is that in making the beam patterns, the input power to the transducer was not monitored, and was assumed to be constant as long as the input voltage was held constant. This assumption may have been false, as shown below. Another reason may have involved wavefront distortion and focusing by the curved surface of the dome.

In order to achieve the peak response at the receiving hydrophone when making the beam patterns, the XU-1347 transducer was moved along the axis of the conical reflector until a peak amplitude was achieved. The position where this peak occurred was the position of maximum focusing of reflections from the interior walls of the dome. Although the input voltage was held constant in this operation, the acoustic impedance load-

CESSION for
IS White Section
C Buff Section
ANNOUNCED
TIFICATION
TRIBUTION/AVAILABILITY CODES
AVAIL SPECIAL
A

ing the XII-1347 changed. This, in turn, gave rise to a change in the input power $P = \frac{V^2}{R_e Z}$ (total). A protion of this loading impedance, Z_t, is dependent on the medium in which the transducer is located. The remainder of the loading impedance is dependent on the reflection from the interior walls of the dome. The portion of the loading impedance which is dependent upon reflections is out of phase with the impedance of the medium, which gives rise to a reduction in the total vector impedance ($\bar{Z}_x = \bar{Z}_o + \bar{Z}_r$).

The acoustic impedance at a point in a medium is defined as the complex ratio of the sound pressure to the particle velocity. For example, in a plane wave propagating in the X direction in a homogeneous medium (the water at Dodge Pond at a particular depth and time can be taken to be a homogeneous body), the variation of pressure with time and distance is:

$$p = P e^{-\alpha x} e^{-j\beta(x-ct)} \tag{1}$$

where p is the instantaneous excess pressure
X is the distance traveled by the wave
P is the initial pressure amplitude
t is time
α is the attenuation constant of the medium
$\beta = W/C$ is the phase constant

Similarly the particle velocity is

$$v = \frac{1}{\rho W}\frac{\partial p}{\partial x} = P\frac{1}{\rho C}\left(1 - j\frac{\alpha C}{W}\right)e^{-\Gamma x} \tag{2}$$

where $\Gamma = \alpha + j\beta$ is the propagation constant
ρ = density of the medium

$$Z_o(x) = \frac{p(x)}{v(x)} = \frac{\rho C}{1 - j\frac{\alpha C}{W}} \tag{3}$$

where Zo is the characteristic impedance of the medium.(Freefield) (see reference (a))

Fig. 16 demonstrates how reflections may change the loading impedance on the transmitting hydrophone.

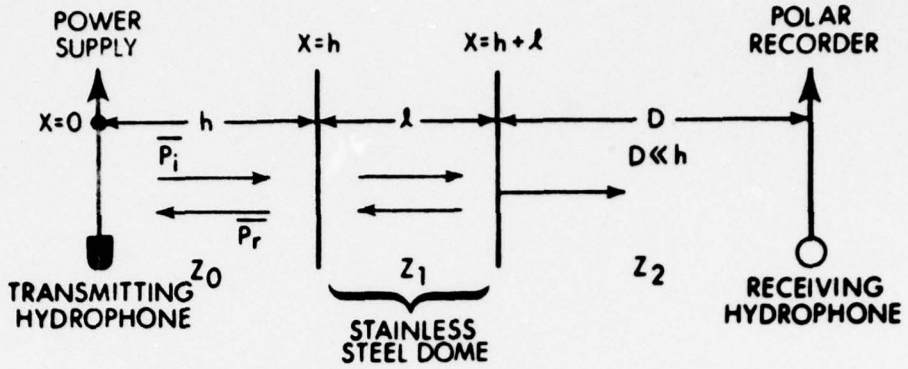

Fig. 16

The acoustic pressure seen by the transmitting transducer, neglecting secondary reflections (or assuming the dome has zero thickness), is:

$$P(x) = \left[P_1 e^{(\alpha - i\beta)x} + P_2 e^{(\alpha + i\beta)(x-h)}\right] e^{i\omega t} \tag{4}$$

$$V(x) = \left[\frac{P_1}{Z_0} e^{(\alpha - i\beta)x} - \frac{P_2}{Z_0} e^{(\alpha + i\beta)(x-h)}\right] e^{i\omega t} \tag{5}$$

$$P(0) = \left[P_1 + P_2 e^{-(\alpha + i\beta)h}\right] e^{i\omega t} \tag{6}$$

$$V(0) = \left[\frac{P_1}{Z_0} - \frac{P_2}{Z_0} e^{-(\alpha + i\beta)h}\right] e^{i\omega t} \tag{7}$$

$$Z_T = \frac{P(0)}{V(0)} = \frac{P_1 + P_2 e^{-(\alpha + i\beta)h}}{\frac{P_1}{Z_0} - \frac{P_2}{Z_0} e^{-(\alpha + i\beta)h}} = Z_0 \frac{P_1 + P_2 e^{-\Gamma h}}{P_1 - P_2 e^{-\Gamma h}} \tag{8}$$

Therefore, as can be observed from the above expressions, the initial pressure and the reflected pressure add vectorily, the reflected pressure being out of phase with the initial pressure. Thus, the loading impedance is less than the characteristic impedance of the medium. As a result, the power input will increase (voltage held constant) when transmitting through the dome, compared to the case when the dome is not present. Also, the pressure level at the receiving hydrophone is greater when the dome is present. (For this to be true, the transmission loss through the dome must be small in order not to counteract the effect of the reflections.) The increased pressure level at the receiving hydrophone gives rise to the pseudo transmission gain observed from the beam patterns. At the higher frequencies of 10, 12 and 14 KC, reference to Table I shows that the pseudo gain disappears due to an increase in the transmission loss, especially in the case of the rubber dome because of its thickness. The effect of the change in input power was thus masked by this increase in transmission loss.

As a result of the previously mentioned change in input power, the apparent transmission loss at the 000° bearing was quite erratic. Now, referring to the transmission loss at the 090° bearing, where the focusing effect of the reflections was not as great, it can be seen that at the lower frequencies the loss in the rubber dome was comparable to that in the reference stainless steel dome. As the frequency was increased, the transmission loss in the rubber dome increased much faster than that in the stainless steel dome.

Table I shows that as far as beam width and side lobe level are concerned, the patterns associated with the stainless steel and rubber domes are in good agreement. It will be noticed that at 3.5 KC and 5 KC there was a considerable increase in beam width compared to the higher frequencies. This is primarily due to the constant size of the projector. The projector used was designed for smaller wave lengths than those encountered at 3.5 and 5 KC. For example, at 5 KC the wave length is approximately one foot, while the major dimension of the projector is 2.5 feet (see diagram of test set-up). From antenna theory, a common rule-of-thumb is that the major dimension of the projector should be at least five wave lengths in order to achieve a narrow beam pattern (15° or less). This rule is not met by the projector used in the test at the previously-mentioned lower frequencies.

Receiving Beam Patterns

Receiving beam patterns were made for bearings of 000°, 090°, and 180° relative to the center of the dome. These tests were performed in a similar manner to those for the transmitting response except that the XU-1347 hydrophone was used for the receiving hydrophone and a J-9 transducer placed in the far field was used for transmitting. The position of the XU-1347 hydrophone within the cone was kept the same as in making the corresponding transmitting patterns. Figures 17 through 22 illustrate the receiving beam patterns for 3.5 and 14 KC for the stainless steel dome. Figures 23 through 28 illustrate the receiving beam patterns for the rubber dome for the above bearings and frequencies.

Comparing the 000° patterns of the stainless steel dome with those of the rubber dome, it is observed that, as with the transmitting patterns, the difference in transmission loss is small at the lower frequencies; but, as the frequency is increased, the transmission loss in the rubber dome increased much faster than in the stainless steel dome. Again, as with the transmitting patterns, there was a pseudo gain through the dome at the lower frequencies.

In making the receiving patterns, the transmitting transducer was maintained at a relatively large distance (18') from the dome surface. Thus, the reflections of the dome cannot be considered as changing the loading impedance on the transmitting projector, as was the case with the transmitting patterns. Therefore, although input power was not monitored, we can postulate that the input power remained considerably more constant than in the case of the transmitting patterns. The principle reason for this is that, in making the transmitting patterns, the distance between the reflecting surface and transmitting transducer was comparatively small (2'). This small distance resulted in very little spreading loss in the reflected energy, whereas in the case of the receiving patterns, the spreading loss is much greater, causing the effect of the reflected wave on the loading impedance to be negligible.

But, due to the curvature of the dome, we can again postulate that at the lower frequencies, where the transmission loss is small, most of the impinging energy is transmitted through the dome. The energy, in passing through the curved section of the dome, is refracted inward toward the projector, causing a focusing effect to occur. This focusing effect then causes the pressure level seen by the receiving hydrophone to be higher than it would be normally without focusing. This, in turn, gives rise to the pseudo gain.

Reference to Table II shows that there was no appreciable difference between the two domes as far as side lobe levels and beam widths are concerned. Comparing the receiving and transmitting beam patterns of both domes, it can be observed that the basic structures of the patterns are the same.

Reflection Measurements

Reflection measurements were made for both the stainless steel and the rubber dome at a bearing of 090°. A J-9 transducer was used as the transmitting source and a Massa 420 hydrophone was used as the receiver. The signal input to the J-9 was taken from a variable digital pulser, the output of which was a pulsed sine wave at the desired frequency. In performing the reflection measurements, the pulser was programmed to give a pulse of 1/2 millisecond duration, at an interval of 1 second. This enabled the Massa hydrophone, which was suspended six feet from the dome's surface, to detect the transmitted pulse and the reflected pulse before a second pulse was transmitted and interferred with the returning reflected pulse (see Fig. 29, below).

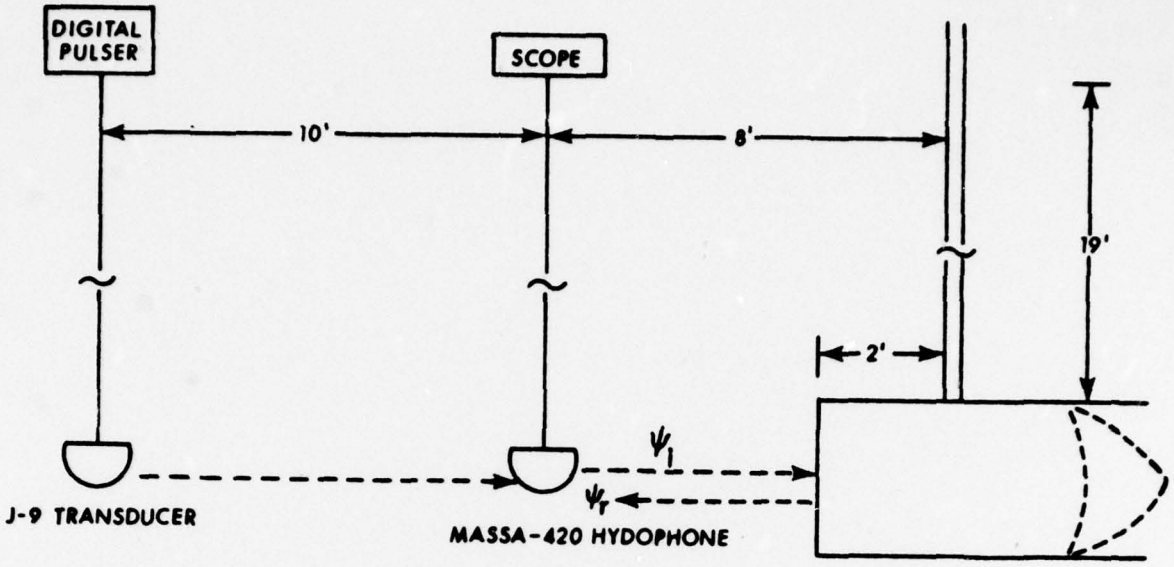

Fig. 29

As can be seen in the sketch, the actual measurements were read from an oscilloscope which was set up to display one complete interval (Figure 30 shows the transmitted and reflected pulses). The amplitudes of the transmitted and reflected pulses, as read from the oscilloscope, were corrected for spreading loss in order to obtain a true measure of the reflection coefficient and make possible a comparison between measured and calculated values of the reflection coefficient (see Fig. 31, below).

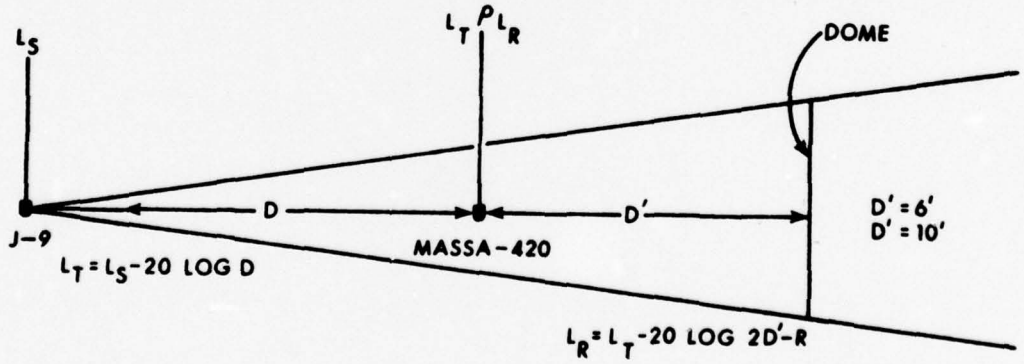

Fig. 31

$$L_R = L_T - 20 \log 2\,D' - R \qquad (9)$$

$$R = L_T - 20 \log 2\,D' \qquad (10)$$

where L_S - is the input source level

L_T - is the relative source level of the impinging pulse measured at the Massa hydrophone.

L_R - is the relative source level of the reflected pulse measured at the Massa hydrophone

R - is the reflection coefficient

Table III gives a comparison of the corrected measured values at a bearing of 090^o, and the related calculated values (see Appendices A and B) for both the stainless steel and rubber domes. (In Appendix A, the expression for the reflection coefficient is derived for a three-layer problem which is an analogy to the stainless steel dome; in Appendix B, the expression for the reflection coefficient is derived for a five-layer problem which is an analogy to the rubber dome.) In Figure 32, their values are plotted. The graph shows that the measured values of the reflection coefficient are lower than the calculated values, 2 db for the stainless steel dome and 1.5 db for the rubber dome. There are basically two reasons for this:

(1) In comparing the measured and calculated reflection coefficients, it was assumed that the measurements were made at normal incidence where maximum reflection occurs. In reality, the impinging energy may have been incident at some small angle (θ) other than 0^o, which would have caused the measured value of the reflection coefficient to be less than the calculated value.

(2) The calculation did not take into consideration the curvature of the dome (see Appendices A and B).

Comparing the reflection coefficients of the stainless steel and rubber domes from Table III, it is observed that the reflection coefficients of the stainless steel dome is approximately 8 db lower than those of the rubber dome, at all frequencies concerned. This apparent superiority of the stainless steel dome as far as reflectivity is concerned is due to two factors:

(1) the difference in the thickness of the domes, and

(2) the particular stainless steel dome did not have bracing to give the skin added strength. The addition of the bracing would have

caused the reflection coefficient to rise substantially. The rubber dome, on the other hand, had structural strength built in by means of the embedded steel wires in the center layer. These imbedded wires were probably the main contributor to the reflection in the rubber dome. This can be illustrated by calculating the reflection coefficient for a mythical pure neoprene rubber dome, of the same thickness as the actual rubber dome, and comparing the reflection coefficients with those of the actual rubber dome used in the test. The results of these calculations are listed below (normal incidence assumed):

Frequency	R actual	R mythical
315 KC	-11.5 db	-50 db
5 KC	-8.8 db	-47 db
8 KC	-6 db	-43 db
10 KC	-4.8 db	-41 db
12 KC	-4.2 db	-37 db
14 KC	-3.7 db	-35 db

It can be seen from the above table that, if a dome could be made of pure neoprene rubber, the reflection from this dome would be negligible since the acoustic impedence of the pure rubber ($Z = \frac{\rho c}{\cos\theta}$) is closely matched to that of water.

Z (Water) = 1.51 g/cm^2 sec Z (neoprene rubber) = 2.1 g/cm^2 sec

From an examination of the calculations in Appendices A and B, a number of interesting facts are apparent. For example, refer to the expression for the stainless steel dome reflection coefficient at normal incidence:

$$|R| = \left[\frac{\left(\frac{\rho_2 c_2}{\rho_1 c_1} - \frac{\rho_1 c_1}{\rho_2 c_2}\right)^2 \sin\left(\frac{2\pi f h}{c_2}\right)^2}{4\cos\left(\frac{2\pi f h}{c_2}\right)^2 + \left(\frac{\rho_2 c_2}{\rho_1 c_1} + \frac{\rho_1 c_1}{\rho_2 c_2}\right)^2 \sin\left(\frac{2\pi f h}{c_2}\right)^2} \right] \qquad (11)$$

The amplitude of the above expression depends not only on the acoustic resistance, but on the thickness of the dome and the frequency of the incident wave. The frequency and thickness dependence are represented in the $\cos\frac{2\pi f h}{c_2}$ and $\sin\frac{2\pi f h}{c_2}$ terms. If the thickness (h) is held constant, the amplitude of the reflection coefficient will go through

a series of alternate maximum and minimum values as a function of frequency. Now, if the frequency is held constant and the thickness is increased, the reflection coefficient will increase. This is demonstrated in Table IV, where the reflection coefficients for stainless steel domes of various thicknesses are listed. For example, the difference between the reflection coefficient of a dome 1/16 inch thick and that of one 1/4 inch thick, at a frequency of 3.5 KC, is 10 db. This is also shown in Figure 32, which is a plot of the reflection coefficient (normal incidence) vs. frequency. The six curves on this plot represent the calculated values of the reflection coefficient for the one-inch rubber dome, and for three different thicknesses (1/16", 1/4" and 3/8") for the stainless steel dome. Also given for comparison are the measured values of the reflection coefficient for the reference stainless steel dome and the one-inch rubber dome. From this figure, it can also be seen that the reflection coefficient of the rubber dome is 2 db better than that of the 1/4" thick stainless steel dome, and 4 db better than a 3/8" thick stainless steel dome, where the 1/4" stainless steel is the type skin which is used for the construction of present sonar domes.

In retrospect, it should be remembered that, when making comparisons between the rubber and stainless steel domes, the stainless steel dome skin tested did not have the internal lattice bracing which is an integral part of an operational stainless steel dome. In turm, the rubber dome tested did have structural strength built in by means of the embedded steel wires. When a prototype of the tested rubber dome is installed on a naval vessel, it will not have internal lattice bracing, which would increase the reflection coefficient, but ubstead will be pressurized to add strength.

CONCLUSIONS

Due to the oversight of not monitoring and keeping constant the input power, no concrete conclusion can be drawn in regard to the transmission loss of either of the domes tested. However, there remain certain general conclusions that may be drawn concerning the trend of transmission loss with increases in frequency. At 3.5 KC and 5 KC, the transmission loss of both domes was relatively low, but as the frequency was increased, the transmission loss in the rubber dome increased faster than that in the stainless steel dome.

A comparison of the transmit and receive beam patterns shows that there was no appreciable deformation in the beam patterns of either

dome, which indicates that the domes are equally good two-way channels.

Reflection measurements show that the reflection coefficient of the rubber dome tested was 10 db higher than that of the reference stainless steel dome skin, and 2 db lower than that calculated for a 1/4" stainless steel dome skin. Taking into account that the stainless steel dome skins in actual use need extensive internal lattice bracing for structual support, which increases the reflection coefficient, and that the rubber dome tested had its strucural strength built in by means of the embedded steel wires, it can be concluded that the rubber dome tested is superior to the 1/4" stainless steel dome skin, and inferior to the 1/16" reference stainless steel dome skin in regard to reflectivity.

J. B. DONALD
Electronic Engineer

REFERENCES

(a) L. Brekhovskikh, Waves in Layered Media, Academic Press, New York, 1960

(b) L. Beranek, Acoustics, McGraw-Hill, New York, 1954

(c) H. Primakoff, Columbia University, "The Acoustic Properties of Domes", Parts I and II Navy Project No. NS-182, 1944

(d) B. F. Goodrich, Intrim Report, "Pressurized Bow Dome of a Cable-Reinforced Rubber Construction For Use With AN/SQX-26 Sonar", Navy Contract NOSR 89483, Sept. 1964

(e) W. L. Weeks, Electromagnetic Theory For Engineering Applications, Uohn Wiley & Sons, Inc., 1964

(f) Calibration of Electroacoustic Transducers, Acoustical Society of America, Dec. 1957

COMPARISON OF STAINLESS STEEL AND RUBBER DOME TRANSMIT BEAM PATTERNS

Frequency (KC)	STAINLESS STEEL DOME			RUBBER DOME		
	Relative Transmission Loss	Beam Width 3 db Down Point	Side Lobe Level	Relative Transmission Loss	Beam Width 3 db Down Point	Side Lobe Level
000° Bearing						
3.5	-1 db	43°	16 db	-.5 db	45°	13 db
5	-2	31°	18	-2	34°	16
8	-.2	14°	16	-2	15°	13
10	.5	13°	14	0	13°	14
12	-.2	12°	12	2	13°	12
14	0	13°	12	1.2	14°	12
090° Bearing						
3.5	0 db	34°	--	1.2 db	35°	--
5	.2	32°	--	.6	32°	--
8	1	13°	14	2	13°	15
10	-.2	13°	17	2.4	14°	13
12	0	12°	15	2.5	13°	13
14	-1	13°	15	3	14°	11

TABLE I

COMPARISON OF STAINLESS STEEL AND RUBBER DOME RECEIVE BEAM PATTERNS

Frequency (KC)	STAINLESS STEEL DOME			RUBBER DOME		
	Relative Transmission Loss	Beam Width 3 db Down Point	Side Lobe Level	Relative Transmission Loss	Beam Width 3 db Down Point	Side Lobe Level
000° Bearing						
3.5	-1 db	51°	14 db	-1.4 db	45°	13 db
5	-2.8	32°	18	-1.4	33°	17
8	-.2	15°	16	1	15°	16
10	-.1	12°	16	3	15°	12
12	-.7	13°	15	2.5	14°	14
14	1	12°	12	2	11°	13
090° Bearing						
3.5	-.8 db	33°	--	.6 db	38°	--
5	-.4	32°	--	2.5	37°	--
8	.4	14°	17	.8	13°	12
10	.2	13°	16	2.8	13°	14
12		13°	15	2.5	14°	13
14	1.6	12°	15	3.2	14°	16

TABLE II

COMPARISON OF CALCULATED AND MEASURED VALUES OF
REFLECTION COEFFICIENT FOR NORMAL INCIDENCE

Frequency (KC)	R (Measured)	R (Calculated)	R (Measured)	R (Calculated)
3.5	-15 db	-21 db	-12.4 db	-11.8 db
5	-18.4 db	-17.6 db	-10.5 db	-9 db
8	-15.5 db	-14 db	- 9.5 db	-6 db
10	-14.8 db	-12 db	- 7 db	-4.8 db
12	-12.5 db	-10.8 db	- 5.6 db	-4.2 db
14	-11.7 db	- 9.8 db	- 4 db	-3.8 db

TABLE III

VARIATION OF REFLECTION COEFFICIENT WITH ANGLE OF INCIDENCE AND THICKNESS

Frequency (KC)	Angle of Incidence	STAINLESS STEEL DOME h(Thickness)=1/16" R (db)	Phase	h=¼" R (db)	Phase	h=3/8" R (db)	Phase	RUBBER DOME h=1" R (db)	Phase
3.5	0°	-21	-85°	-9.3	-70°	-6.5	-62°	-11.5	-62°
	15°	-21.3	-85°	-9.6	-71°	-6.8	-63°	-11.9	-63°
	30°	-22.2	-86	-11.4	-73°	-7.5	-65°	-12.8	-65°
	45°	-23.8	-87°	-12	-76°	-8.8	-69°	-14.3	-70°
	60°	-26.5	-88°	-14.9	-80°	-11.4	-76°	-17	-77°
	75°	-31	-89°	-19	-86°	-15.4	-84°	-21.7	-84°
	90°	0	180°	0	180°	0	180°	0	180°
5	0°	-17.6	-82°	-6.8	-63°	-4.3	-52°	-9.8	-51°
	15°	-18.4	-83°	-7.2	-64°	-4.5	-53°	-9.2	-52°
	30°	-19	-84°	-7.7	-66°	-5	-56°	-9.8	-56°
	45°	-20.3	-85°	-9	-70°	-6.4	-62°	-11.5	-62°
	60°	-23.5	-86°	-11.7	-76°	-8.6	-70°	-12	-71°
	75°	-28	-88°	-15.8	-84°	-12.5	-81°	-18.5	-82°
8	0°	-14	-78°	-4	-51°	-2.2	-39°	-6	-30°
	15°	-14.5	-79°	-4.2	-52°	-2.3	-40°	-6.2	-32°
	30°	-14.9	-80°	-4.7	-55°	-2.7	-43°	-6.7	-37°
	45°	-16.5	-82°	-5.8	-61°	-3.6	-50°	-8	-47°
	60°	-20	-84°	-8	-69°	-5 4	-60°	-10.2	-60°
	75°	-23.8	-87°	-12	-81°	-8.8	-76°	-14.6	-77°
10	0°	-12	-76°	-3	-45°	-1.5	-33°	-4.8	-18°
	15°	-12.4	-76°	-3.1	-46°	-1.6	-34°	-5	-20°
	30°	-13.8	-77°	-3.5	-49°	-1.8	-37°	-5.5	-26°
	45°	-14.9	-80°	-4.5	-55°	-2.5	-44°	-6.6	-36°
	60°	-17.6	-83°	-6.5	-64°	-4	-55°	-8.6	-53°
	75°	-21.8	-87°	-10.2	-78°	-7.2	-73°	-12.7	-74°
12	0°	-10.7	-73°	-2.3	-39°	-1.2	-28°	-4.2	-6°
	15°	-11.1	-73°	-2.4	-40°	-1.2	-29°	-4.3	-9°
	30°	-11.7	-75°	-2.7	-43°	-1.3	-32°	-4.6	-16°
	45°	-13.8	-78°	-3.6	-50°	-1.8	-38°	-5.5	-28°
	60°	-15.8	-82°	-5.4	-60°	- .3	-50°	-7.7	-46°
	75°	-20.4	-86°	-9.8	-76°	-5.9	-70°	-11.3	-71°
14	0°	- 9.3	-70°	-1.6	-35°	- .9	-25°	-3.7	+5°
	15°	- 9.3	-71°	-1.7	-36°	-1	-26°	-3.8	+3°
	30°	-11.4	-73°	-2 1	-39°	-1.2	-29°	-4.2	-6°
	45°	-12	-76°	-2.8	-46°	-1.3	-35°	-4.8	-20°
	60°	-14.9	-80°	-4.3	-56°	-2.4	-46°	-6.5	-40°
	75°	-19	-86°	-7.5	-74°	-4.7	-68°	-10.2	-68°

TABLE IV

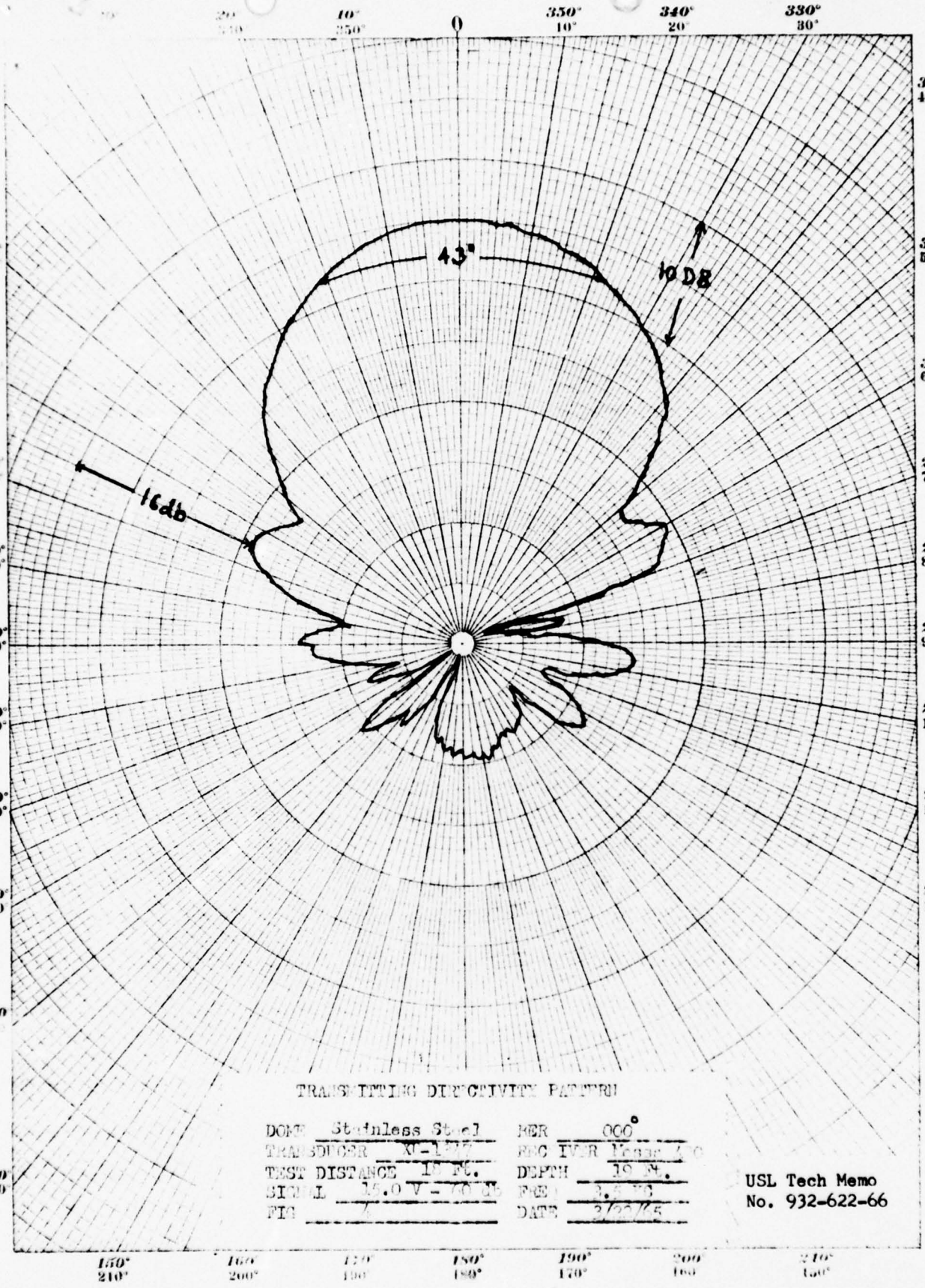

TRANSMITTING DIRECTIVITY PATTERN

DOME Stainless Steel
TRANSDUCER X-[illegible]
TEST DISTANCE 10 Ft.
SIGNAL 15.0 V - 70 [illegible]
FIG 7

MER 000°
REC IVER [illegible]
DEPTH 10 M.
FRE [illegible]
DATE 3/[illegible]/65

USL Tech Memo
No. 932-622-66

CODEX BOOK COMPANY, INC. NORWOOD, MASSACHUSETTS
PRINTED IN U.S.A.
NO. 324 POLAR CO-ORDINATE.

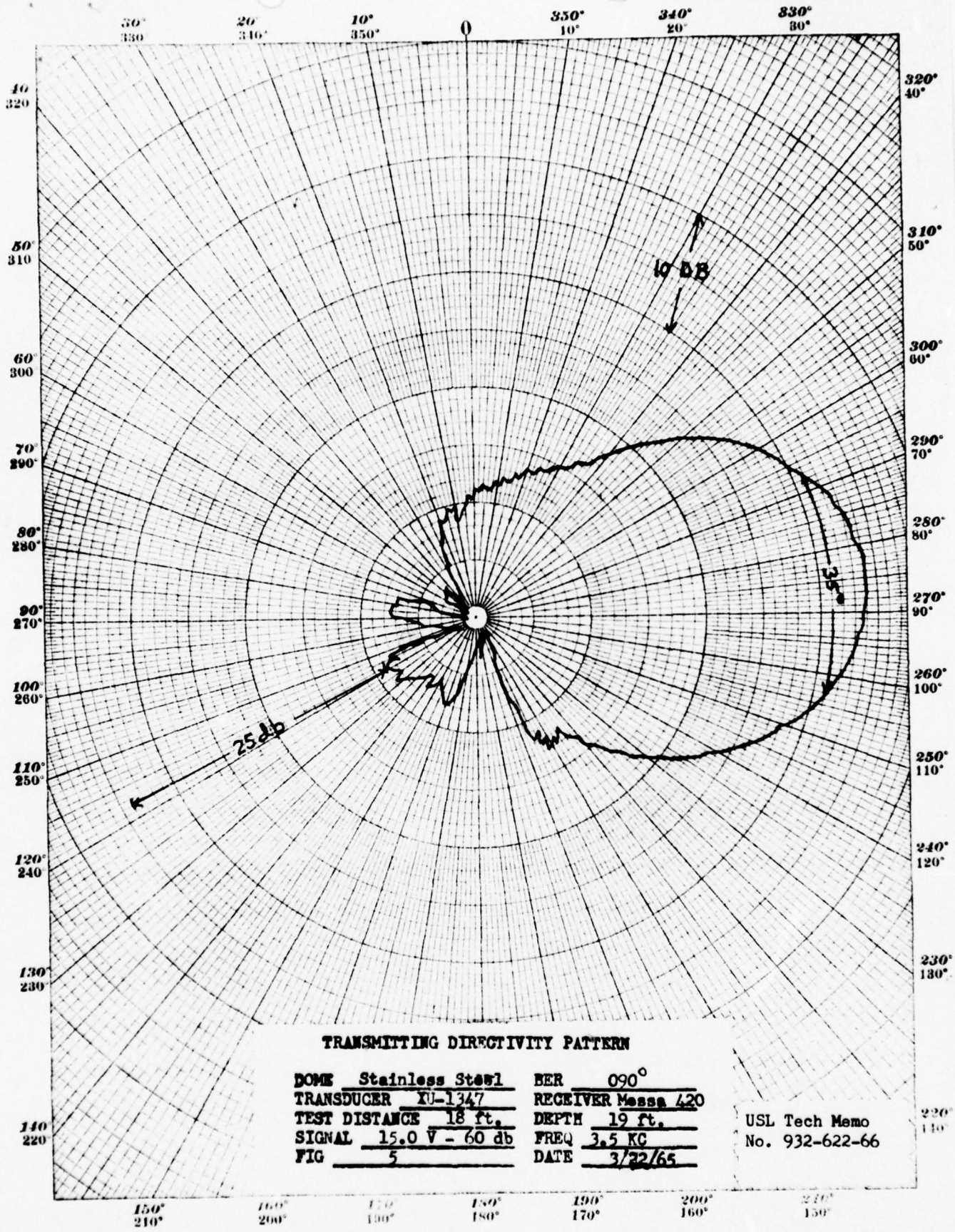

TRANSMITTING DIRECTIVITY PATTERN

DOME	Stainless Steel	BER	090°
TRANSDUCER	XU-1347	RECEIVER	Massa 420
TEST DISTANCE	18 ft.	DEPTH	19 ft.
SIGNAL	15.0 V - 60 db	FREQ	3.5 KC
FIG	5	DATE	3/22/65

USL Tech Memo
No. 932-622-66

COMPANY, INC. NORWOOD, MASSACHUSETTS
PRINTED IN U.S.A.
NO 3124. POLAR CO-ORDINATE.

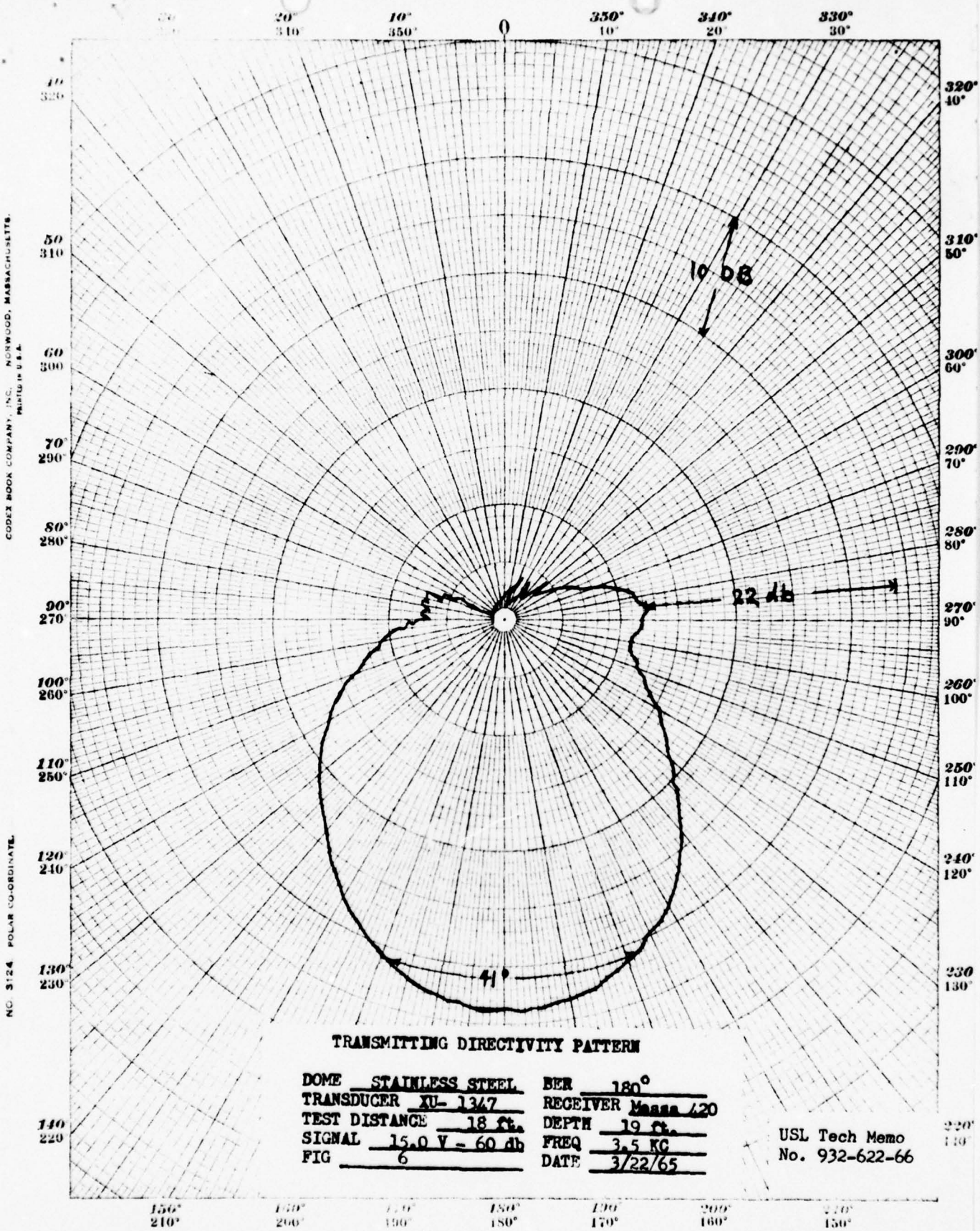

CODEX BOOK COMPANY, INC. NORWOOD, MASSACHUSETTS. PRINTED IN U.S.A.

NO. 3124 POLAR CO-ORDINATE.

TRANSMITTING DIRECTIVITY PATTERN

DOME	STAINLESS STEEL	BER	180°
TRANSDUCER	XU- 1347	RECEIVER	Massa 420
TEST DISTANCE	18 ft.	DEPTH	19 ft.
SIGNAL	15.0 V - 60 db	FREQ	3.5 KC
FIG	6	DATE	3/22/65

USL Tech Memo
No. 932-622-66

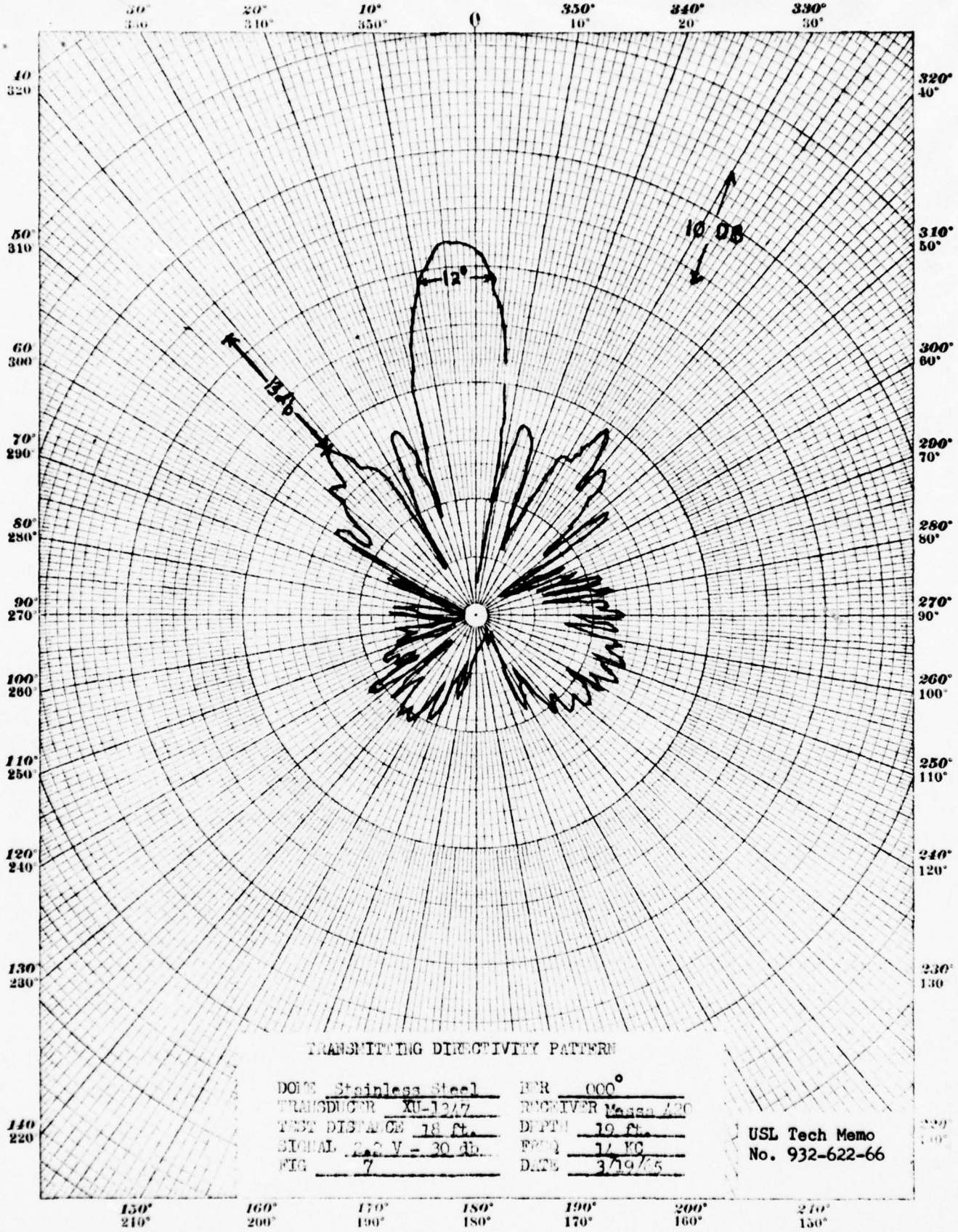

TRANSMITTING DIRECTIVITY PATTERN

DOME	Stainless Steel	BFR	000°
TRANSDUCER	XU-1247	RECEIVER	Massa A30
TEST DISTANCE	18 ft.	DEPTH	19 ft.
SIGNAL	2.2 V - 30 db	FREQ	14 KC
FIG	7	DATE	3/9/65

USL Tech Memo
No. 932-622-66

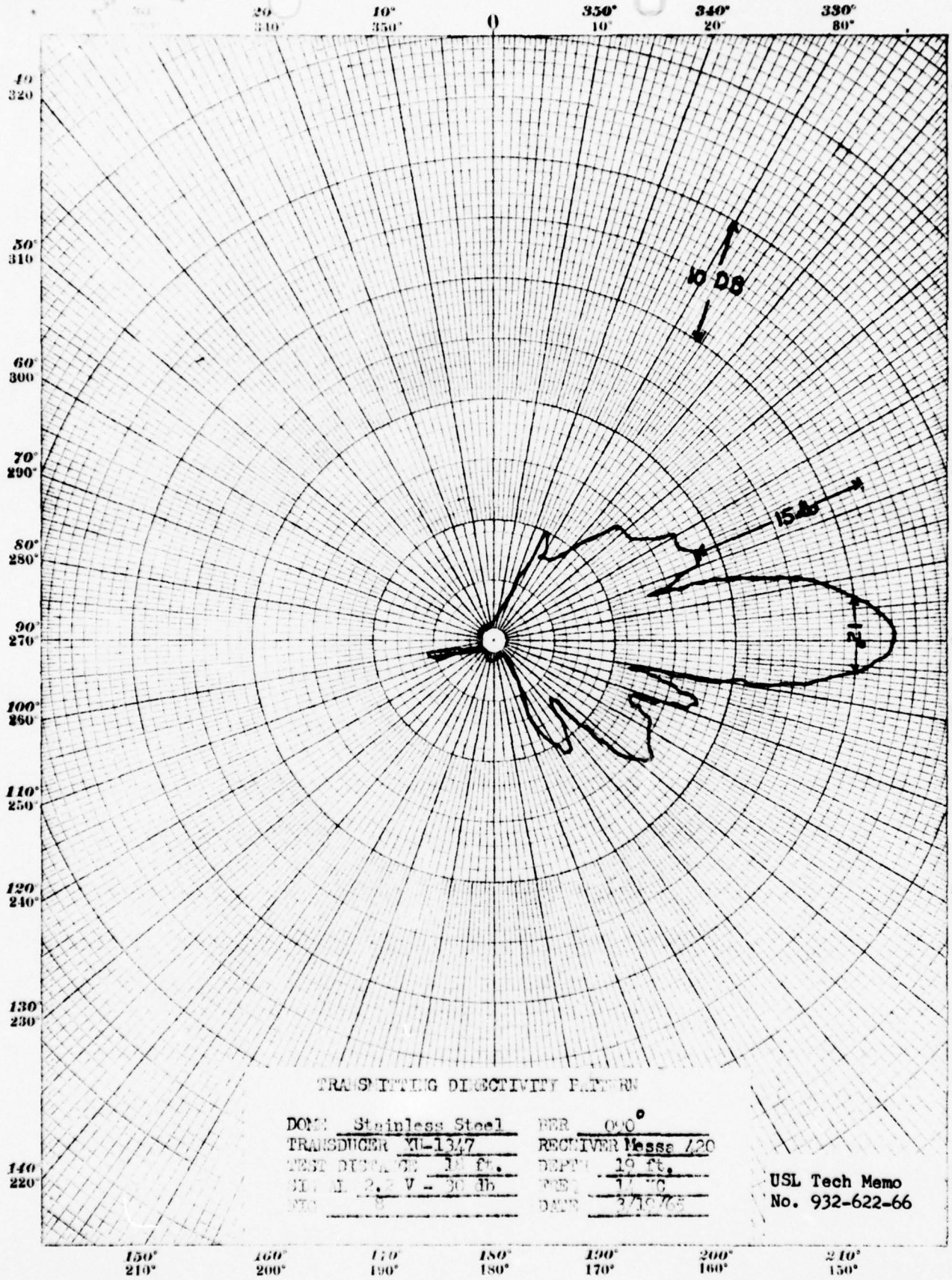

TRANSMITTING DIRECTIVITY PATTERN

DOME	Stainless Steel	BEAM	000°
TRANSDUCER	XL-1347	RECEIVER	Hessa 420
TEST DISTANCE	10 ft.	DEPTH	10 ft.
FREQ.	2. V - 20 db	RANGE	17 ft.
NOTES		DATE	3/16/66

USL Tech Memo
No. 932-622-66

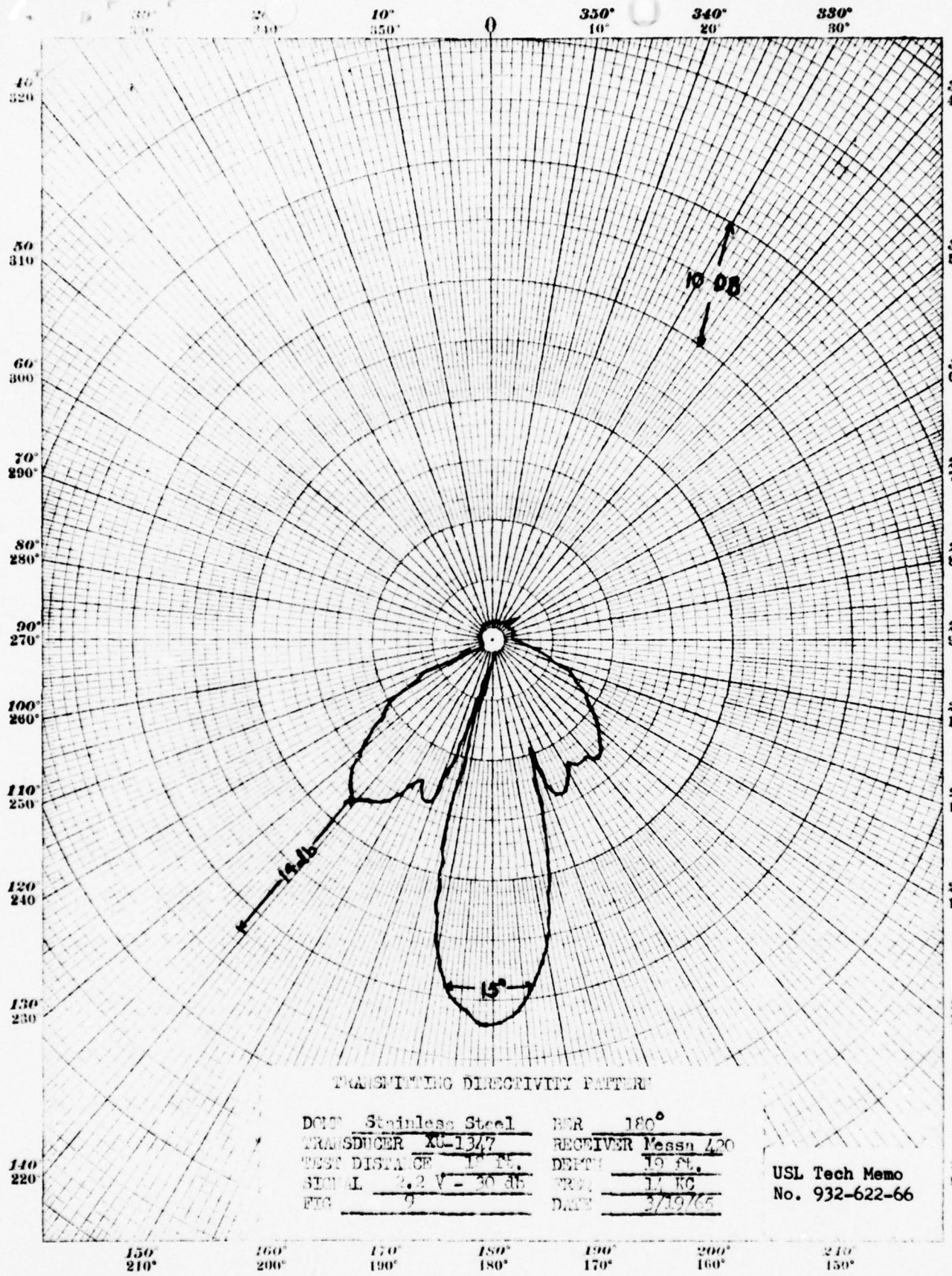

TRANSMITTING DIRECTIVITY PATTERN

DOT	Stainless Steel	BEAM	180°
TRANSDUCER	XC-1347	RECEIVER	Nessa 420
TEST DISTANCE	15 Ft.	DEPTH	19 Ft.
SIGNAL	2.2 V - 30 dB	FREQ	14 KC
FIG	9	DATE	3/19/65

USL Tech Memo
No. 932-622-66

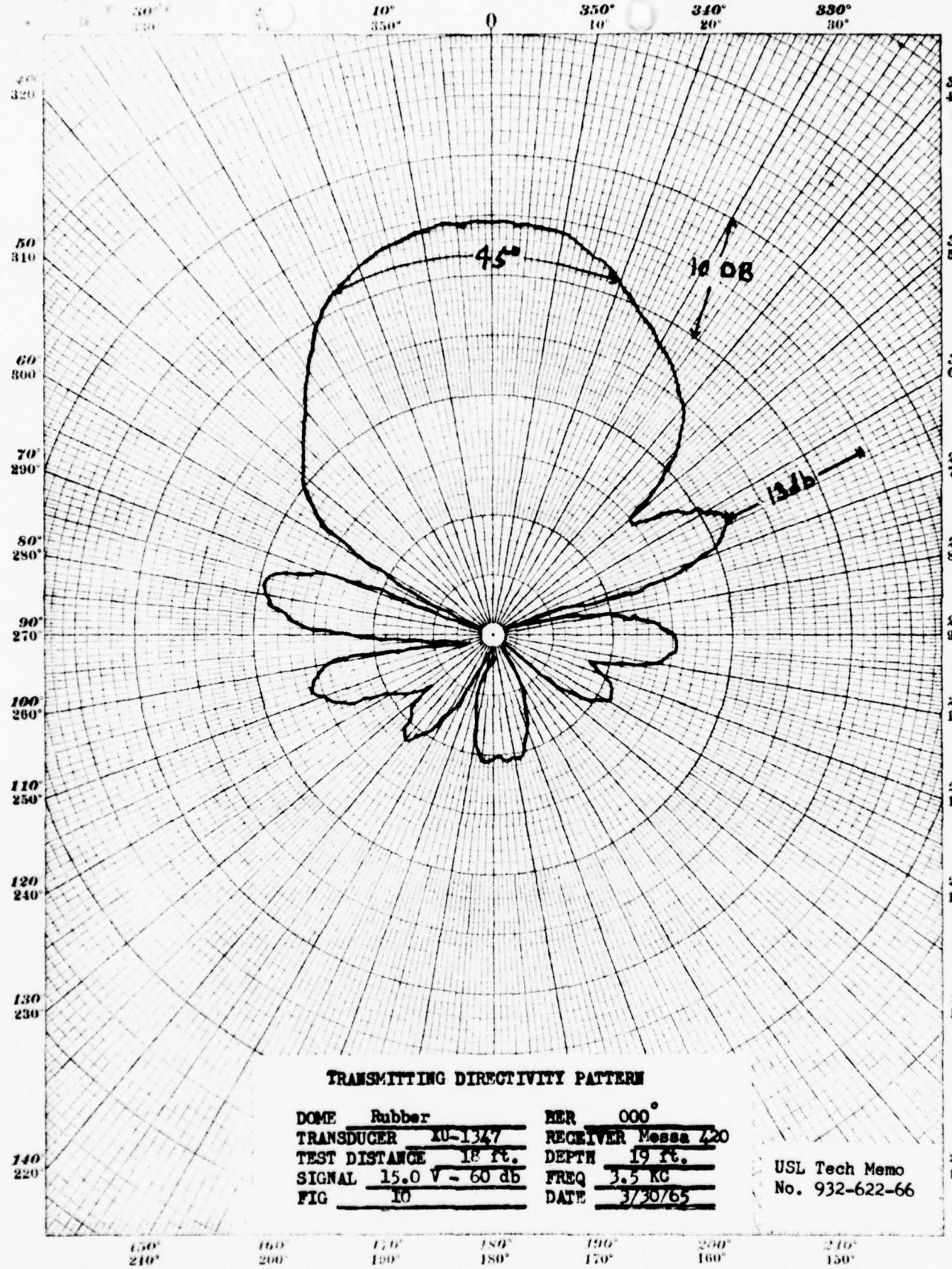

TRANSMITTING DIRECTIVITY PATTERN

DOME	Rubber	BER	000°
TRANSDUCER	XU-1347	RECEIVER	Messa 420
TEST DISTANCE	18 ft.	DEPTH	19 ft.
SIGNAL	15.0 V - 60 db	FREQ	3.5 KC
FIG	10	DATE	3/30/65

USL Tech Memo
No. 932-622-66

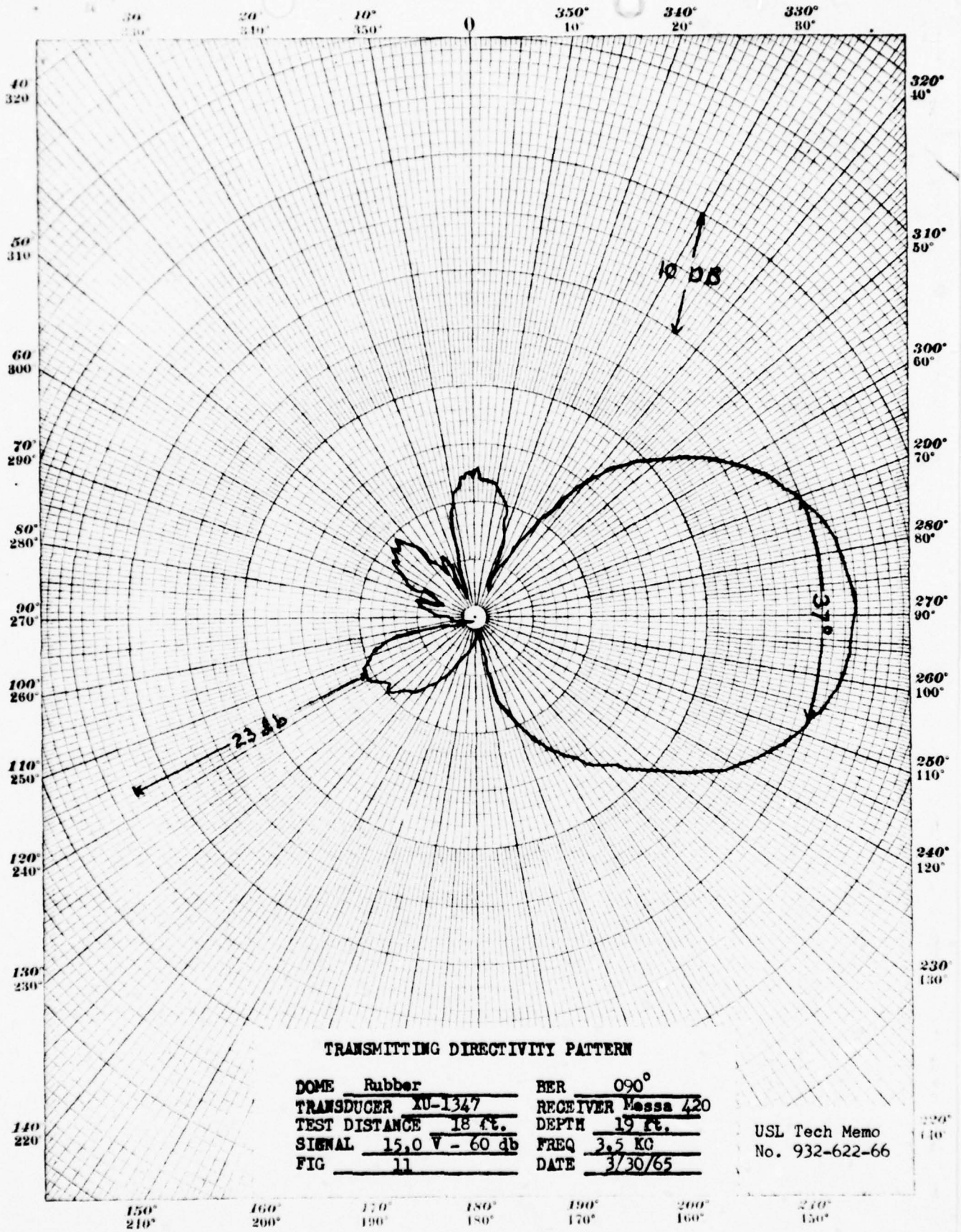

TRANSMITTING DIRECTIVITY PATTERN

DOME	Rubber	BER	090°
TRANSDUCER	XU-1347	RECEIVER	Massa 420
TEST DISTANCE	18 ft.	DEPTH	19 ft.
SIGNAL	15.0 V - 60 db	FREQ	3.5 KC
FIG	11	DATE	3/30/65

USL Tech Memo
No. 932-622-66

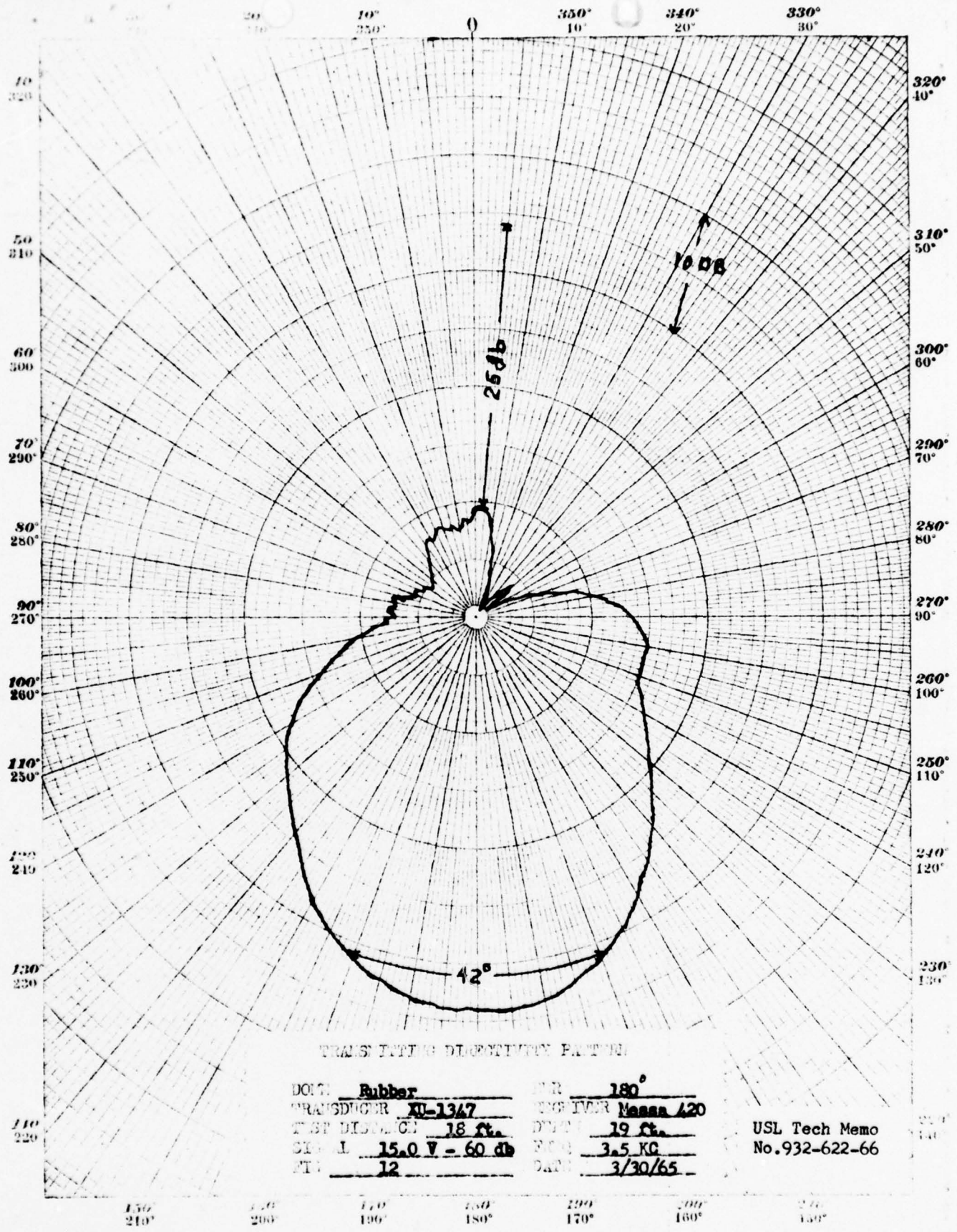

TRANSMITTING DIRECTIVITY PATTERN

DOME	Rubber	BEAM	180°
TRANSDUCER	XU-1347	RECEIVER	Massa 420
TEST DISTANCE	18 ft.	DIST.	19 ft.
SIGNAL	15.0 V - 60 db	FREQ.	3.5 KC
CAL.	12	DATE	3/30/65

USL Tech Memo
No.932-622-66

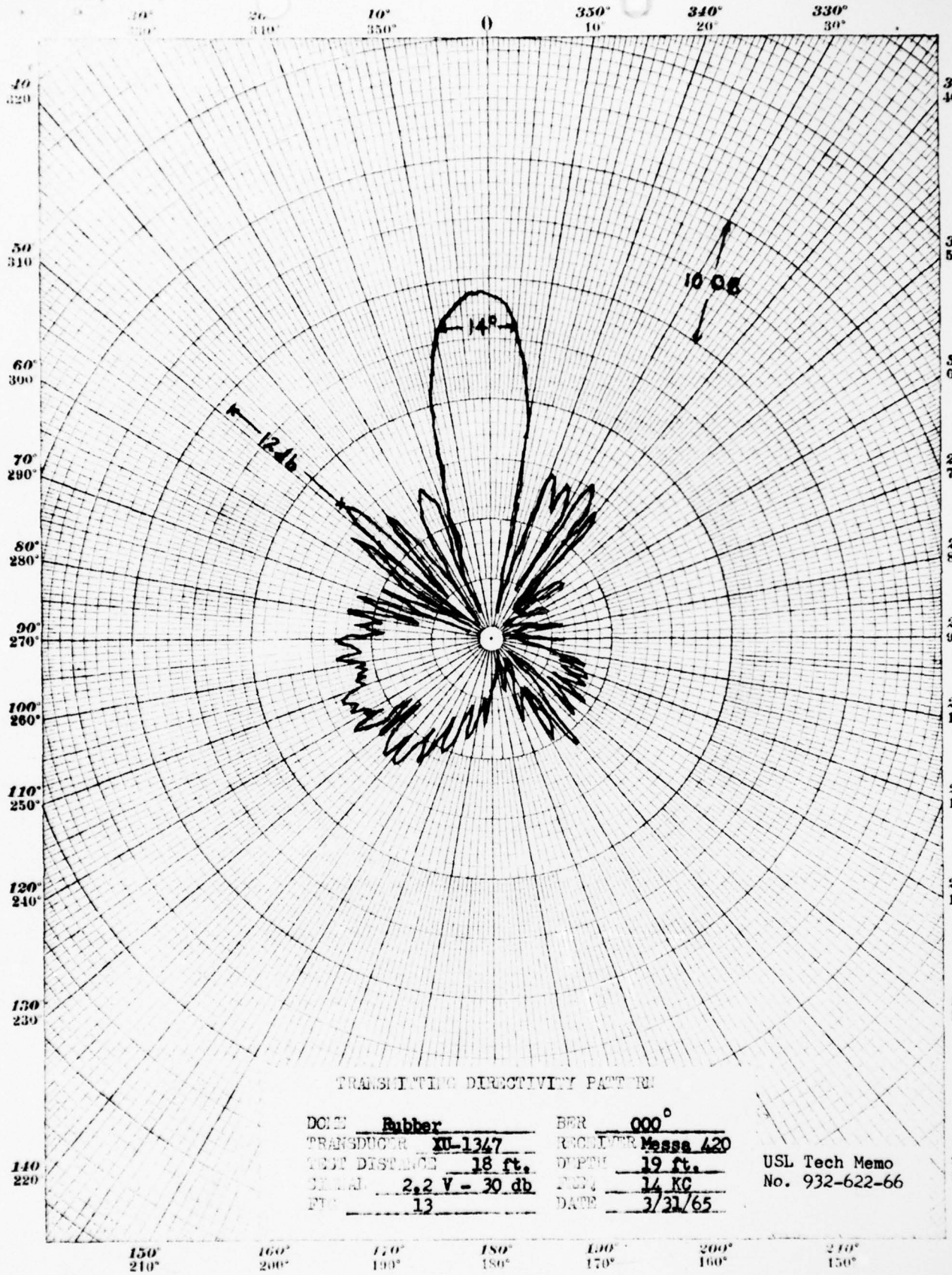

TRANSMITTING DIRECTIVITY PATTERN

DOME: Rubber
TRANSDUCER: XU-1347
TEST DISTANCE: 18 ft.
SIGNAL: 2.2 V - 30 db
FT: 13

BRG: 000°
RECEIVER: Massa 420
DEPTH: 19 ft.
FREQ: 14 KC
DATE: 3/31/65

USL Tech Memo
No. 932-622-66

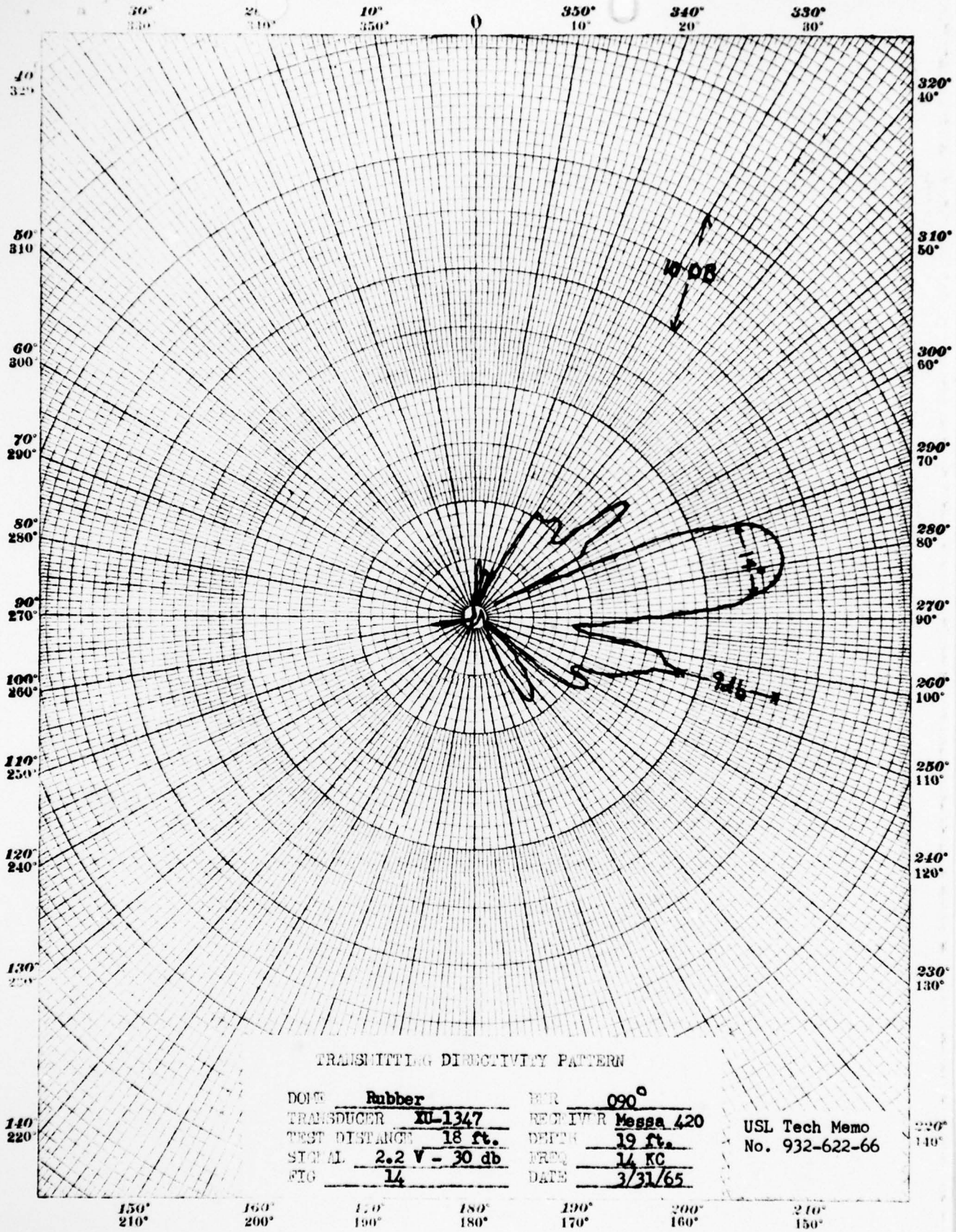

TRANSMITTING DIRECTIVITY PATTERN

DOME	Rubber	BEAM	090°
TRANSDUCER	XU-1347	RECEIVER	Messa 420
TEST DISTANCE	18 ft.	DEPTH	19 ft.
SIGNAL	2.2 V - 30 db	FREQ	14 KC
FIG	14	DATE	3/31/65

USL Tech Memo
No. 932-622-66

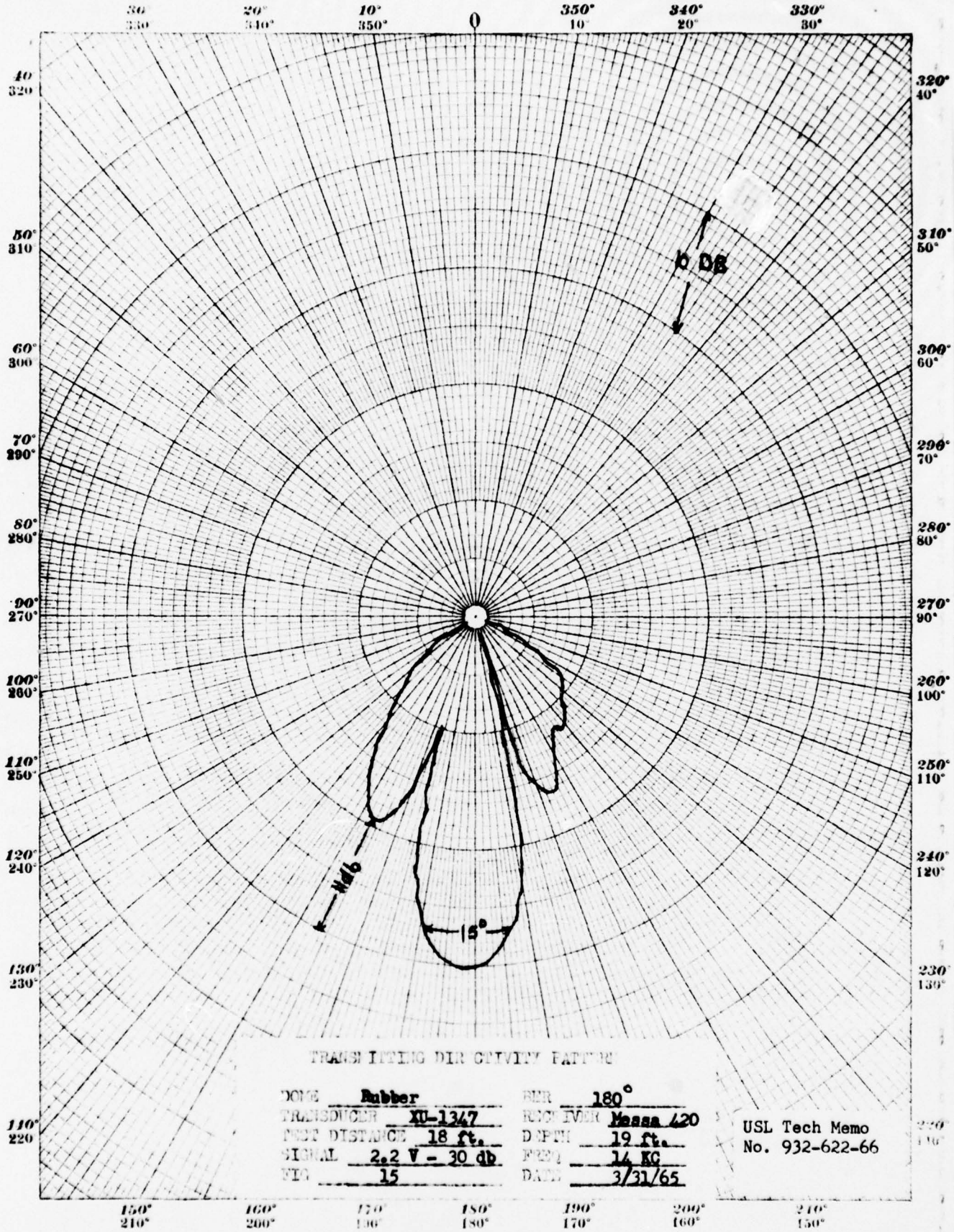

TRANSMITTING DIRECTIVITY PATTERN

DOME	Rubber	BEAM	180°
TRANSDUCER	XU-1347	RECEIVER	Massa 420
TEST DISTANCE	18 ft.	DEPTH	19 ft.
SIGNAL	2.2 V - 30 db	FREQ	14 KC
FIG	15	DATE	3/31/65

USL Tech Memo
No. 932-622-66

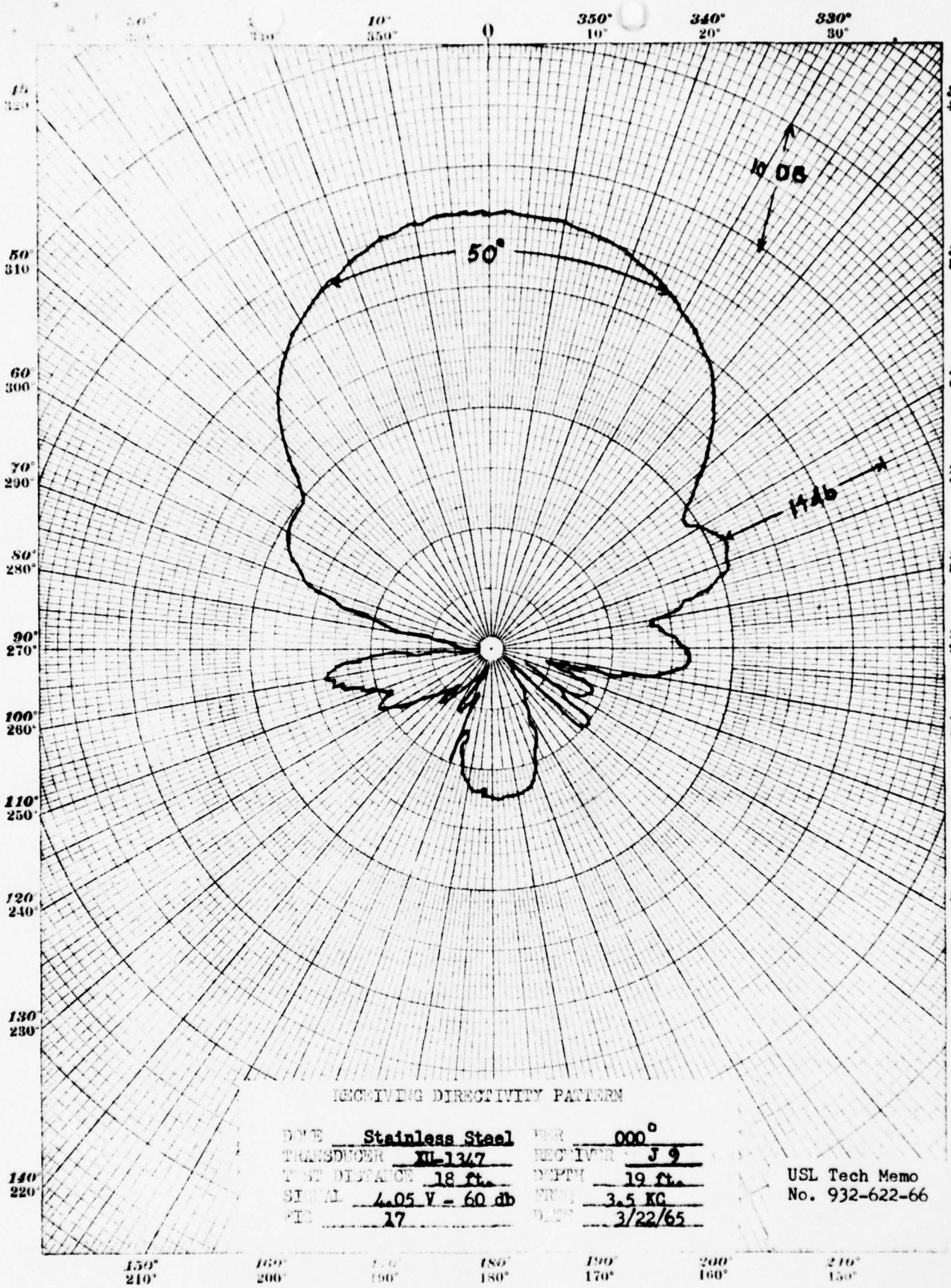

RECEIVING DIRECTIVITY PATTERN

DOME	Stainless Steel	PIER	000°
TRANSDUCER	XU-1347	RECEIVER	J 9
TEST DISTANCE	18 ft.	DEPTH	19 ft.
SIGNAL	4.05 V - 60 db	FREQ	3.5 KC
PI	17	DATE	3/22/65

USL Tech Memo
No. 932-622-66

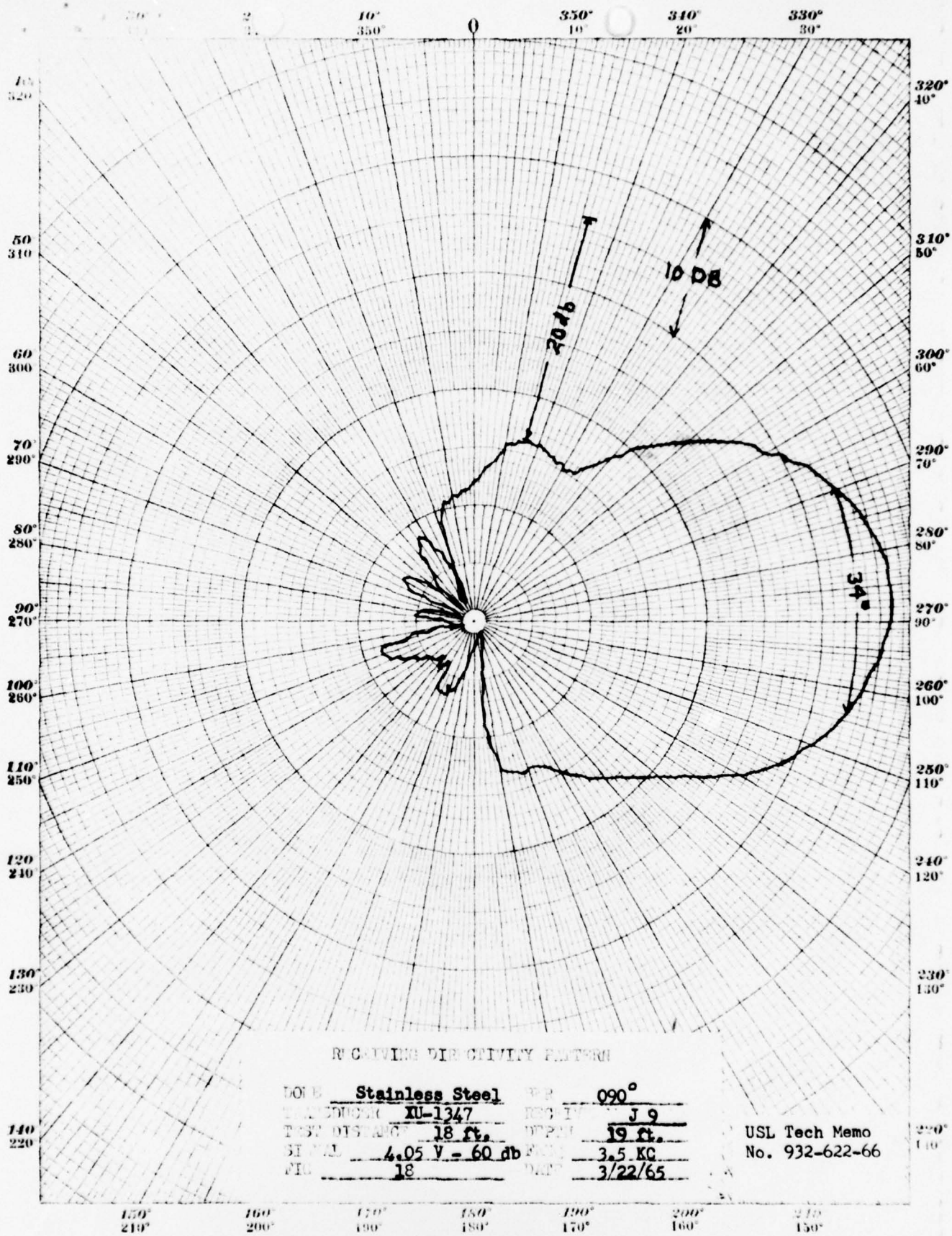

RECEIVING DIRECTIVITY PATTERN

DOME	Stainless Steel		090°
TRANSDUCER	XU-1347		J 9
TEST DISTANCE	18 ft.		19 ft.
SIGNAL	4.05 V - 60 db		3.5 KC
FIG	18		3/22/65

USL Tech Memo
No. 932-622-66

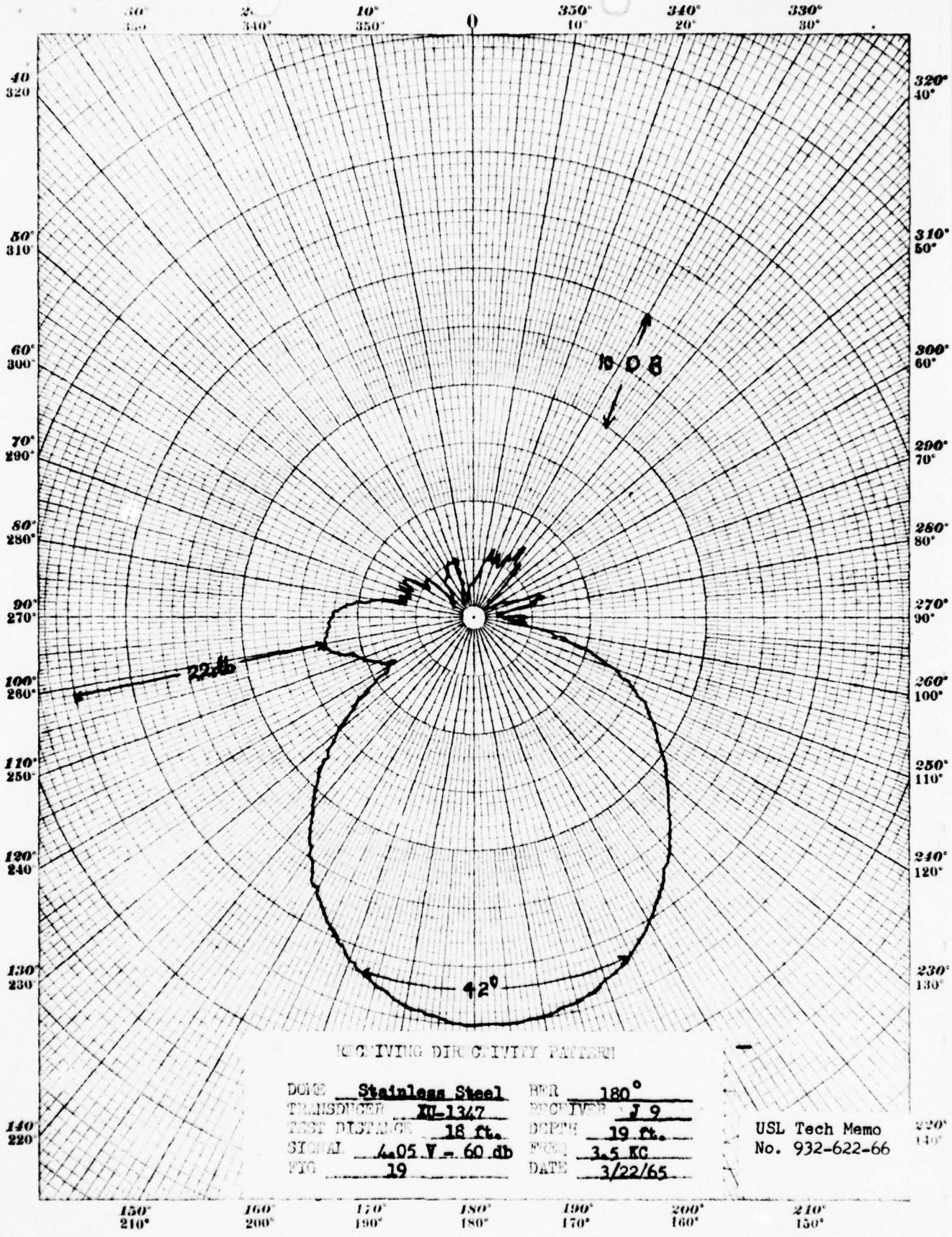

RECEIVING DIRECTIVITY PATTERN

DOME	Stainless Steel	BEAR	180°
TRANSDUCER	XU-1347	RECEIVER	J 9
TEST DISTANCE	18 ft.	DEPTH	19 ft.
SIGNAL	4.05 V - 60 db	FREQ	3.5 KC
FTG	19	DATE	3/22/65

USL Tech Memo
No. 932-622-66

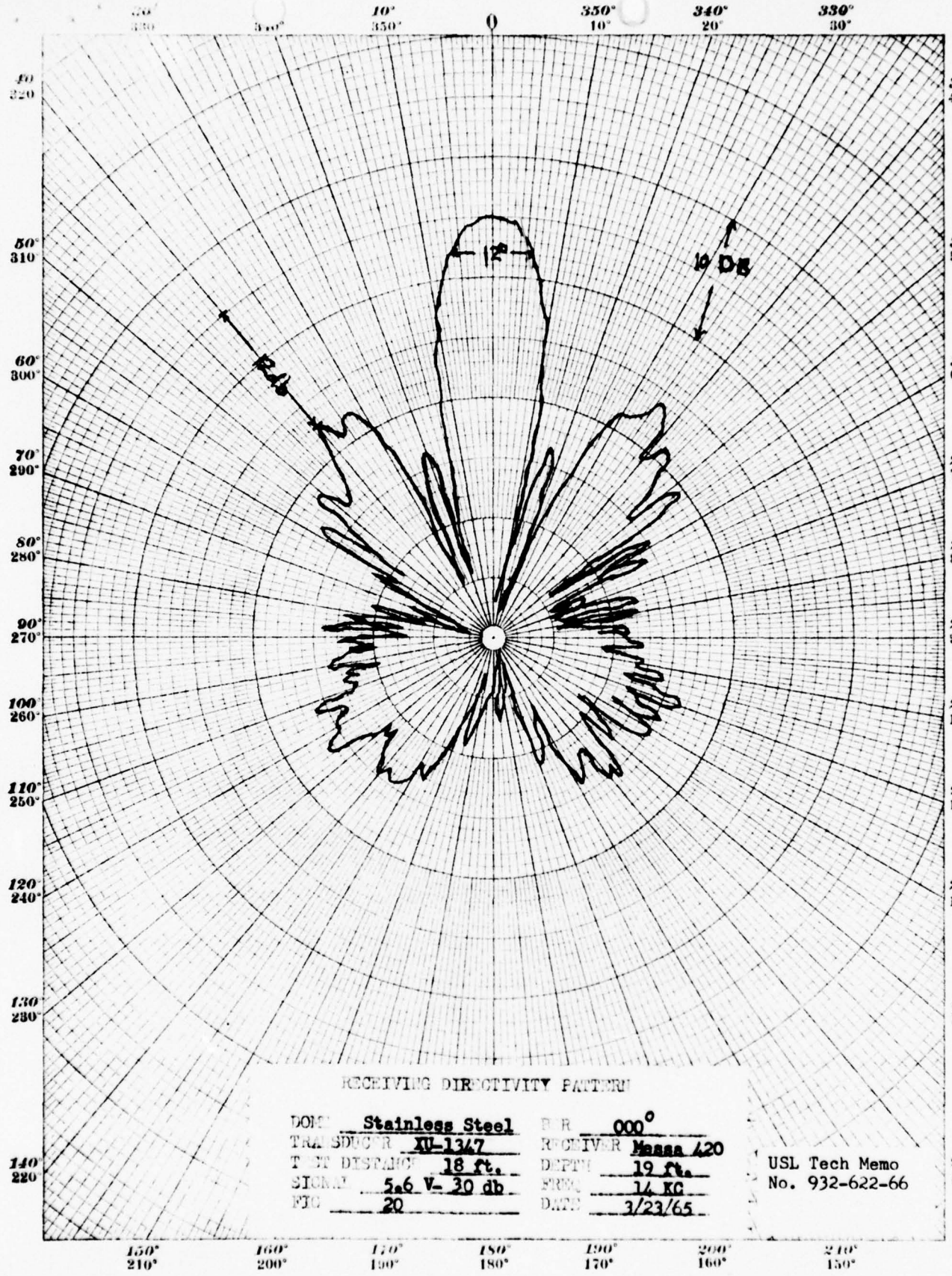
0
10°
350°
340°
20°
330°
30°
320°
40°
310°
50°
300°
60°
290°
70°
280°
80°
270°
90°
260°
100°
250°
110°
240°
120°
230°
130°
220°
140°
210°
150°
200°
160°
190°
170°
180°
12°
10 DB
RECEIVING DIRECTIVITY PATTERN
DOME Stainless Steel
TRANSDUCER XU-1347
TEST DISTANCE 18 ft.
SIGNAL 5.6 V- 30 db
FIG 20
BR 000°
RECEIVER Massa 420
DEPTH 19 ft.
FREQ. 14 KC
DATE 3/23/65
USL Tech Memo
No. 932-622-66

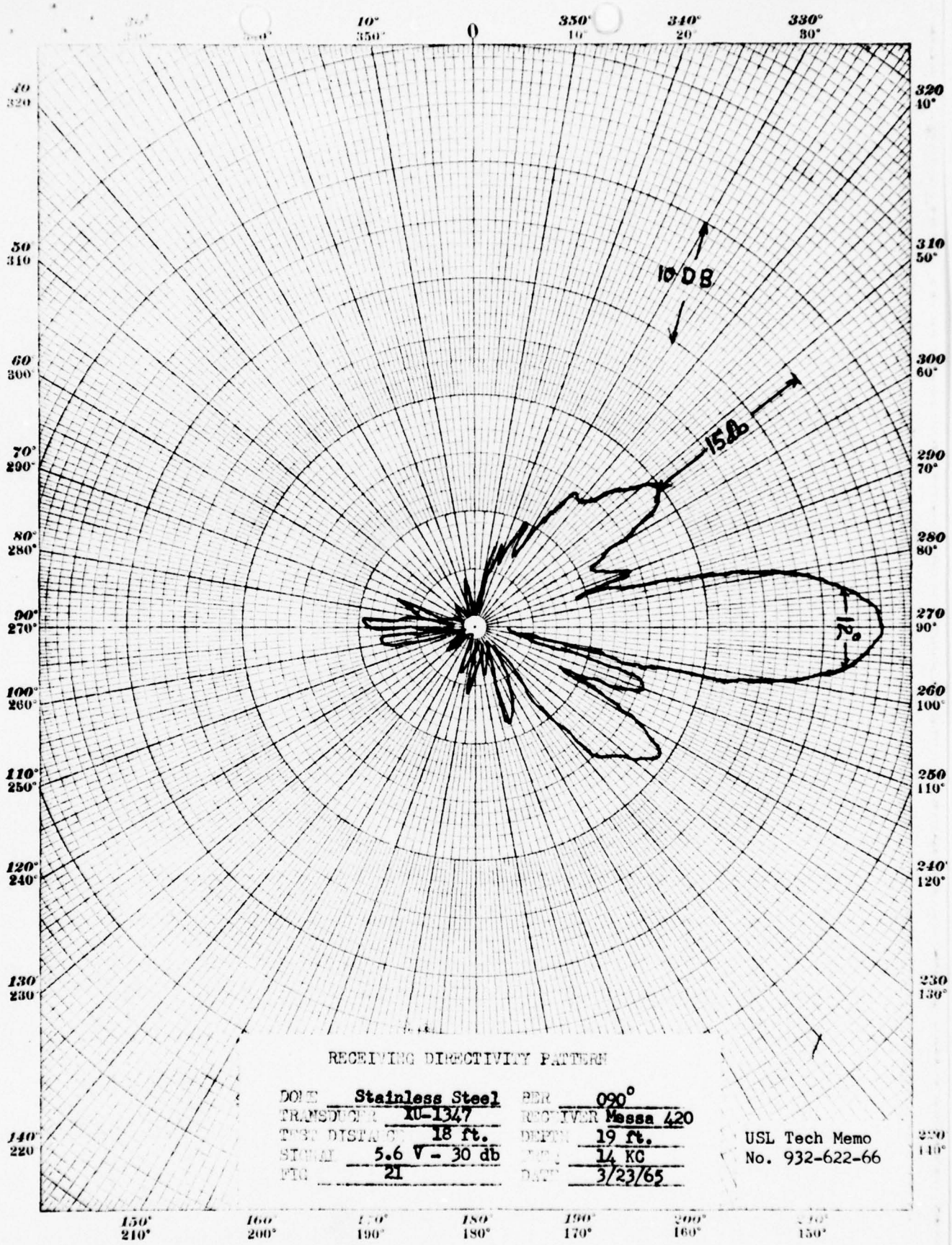

RECEIVING DIRECTIVITY PATTERN

DOME	Stainless Steel	BEAM	090°
TRANSDUCER	XU-1347	RECEIVER	Massa 420
TEST DISTANCE	18 ft.	DEPTH	19 ft.
SIGNAL	5.6 V - 30 db	FREQ.	14 KC
FIG	21	DATE	3/23/65

USL Tech Memo
No. 932-622-66

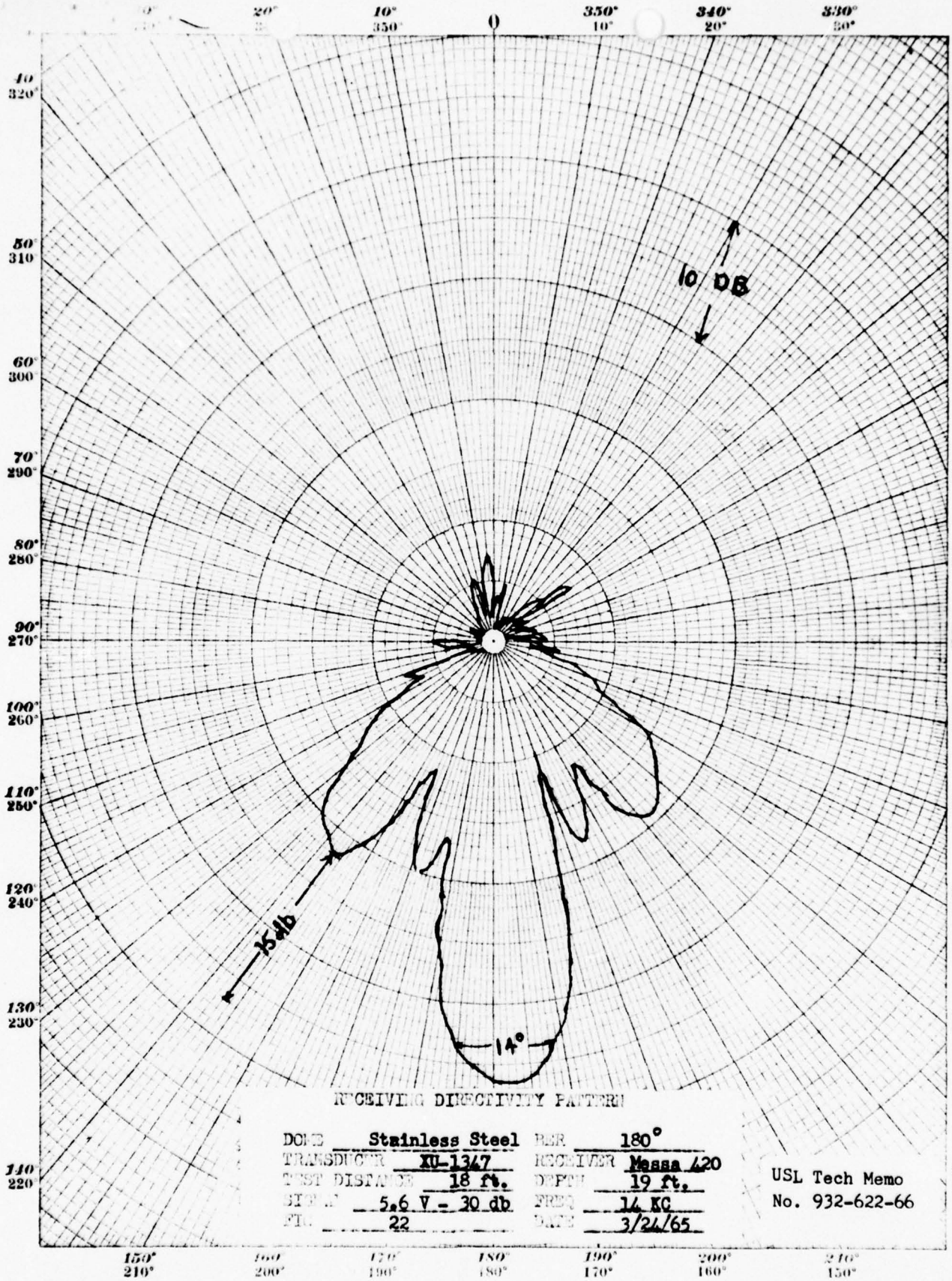

RECEIVING DIRECTIVITY PATTERN

DOME	Stainless Steel	BEAR	180°
TRANSDUCER	XU-1347	RECEIVER	Massa 420
TEST DISTANCE	18 ft.	DEPTH	19 ft.
SIGNAL	5.6 V - 30 db	FREQ	14 KC
FIG.	22	DATE	3/24/65

USL Tech Memo
No. 932-622-66

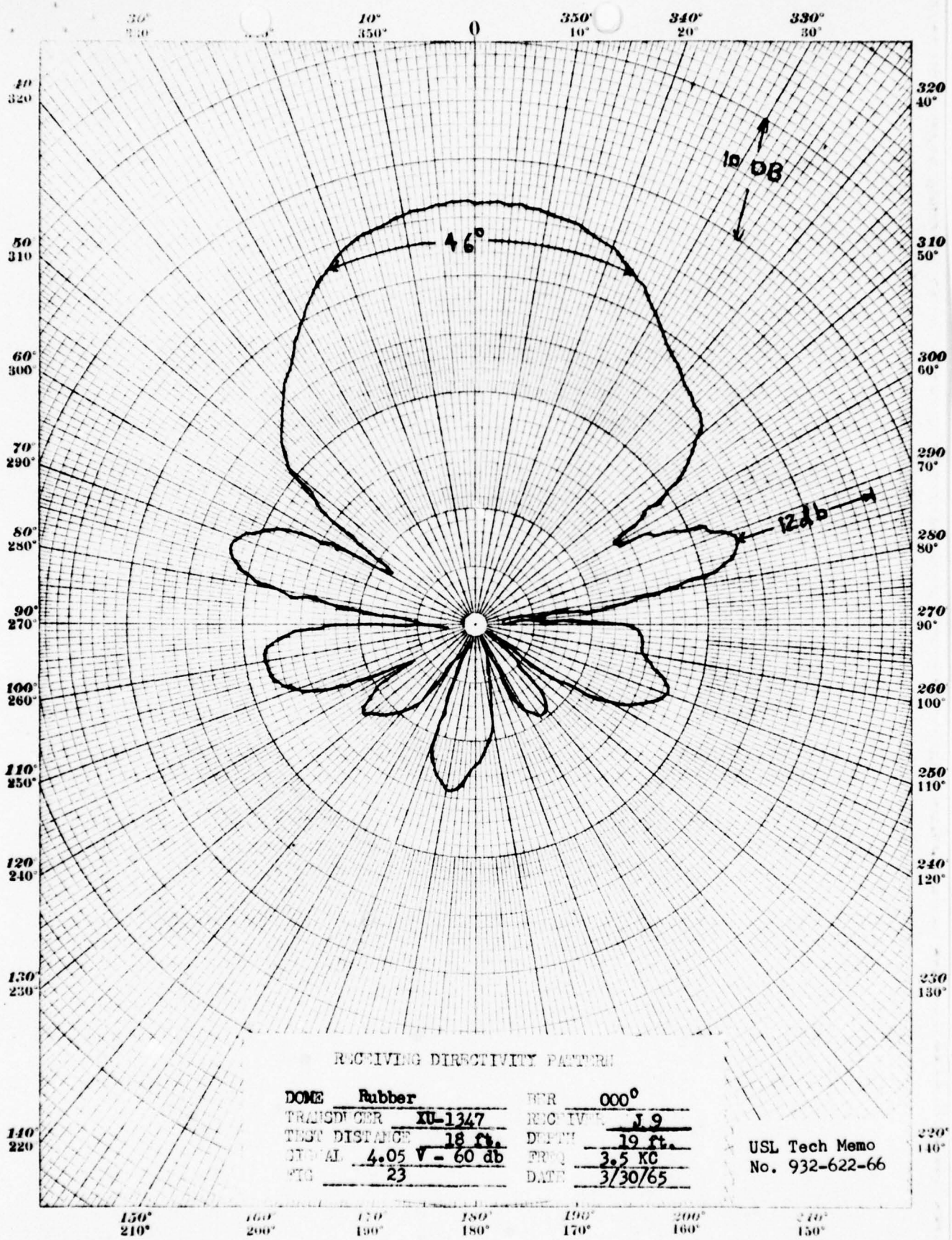

RECEIVING DIRECTIVITY PATTERN

DOME	Rubber	BEAR	000°
TRANSDUCER	XU-1347	RECEIVER	J 9
TEST DISTANCE	18 ft.	DEPTH	19 ft.
SIGNAL	4.05 V - 60 db	FREQ	3.5 KC
NOTES	23	DATE	3/30/65

USL Tech Memo
No. 932-622-66

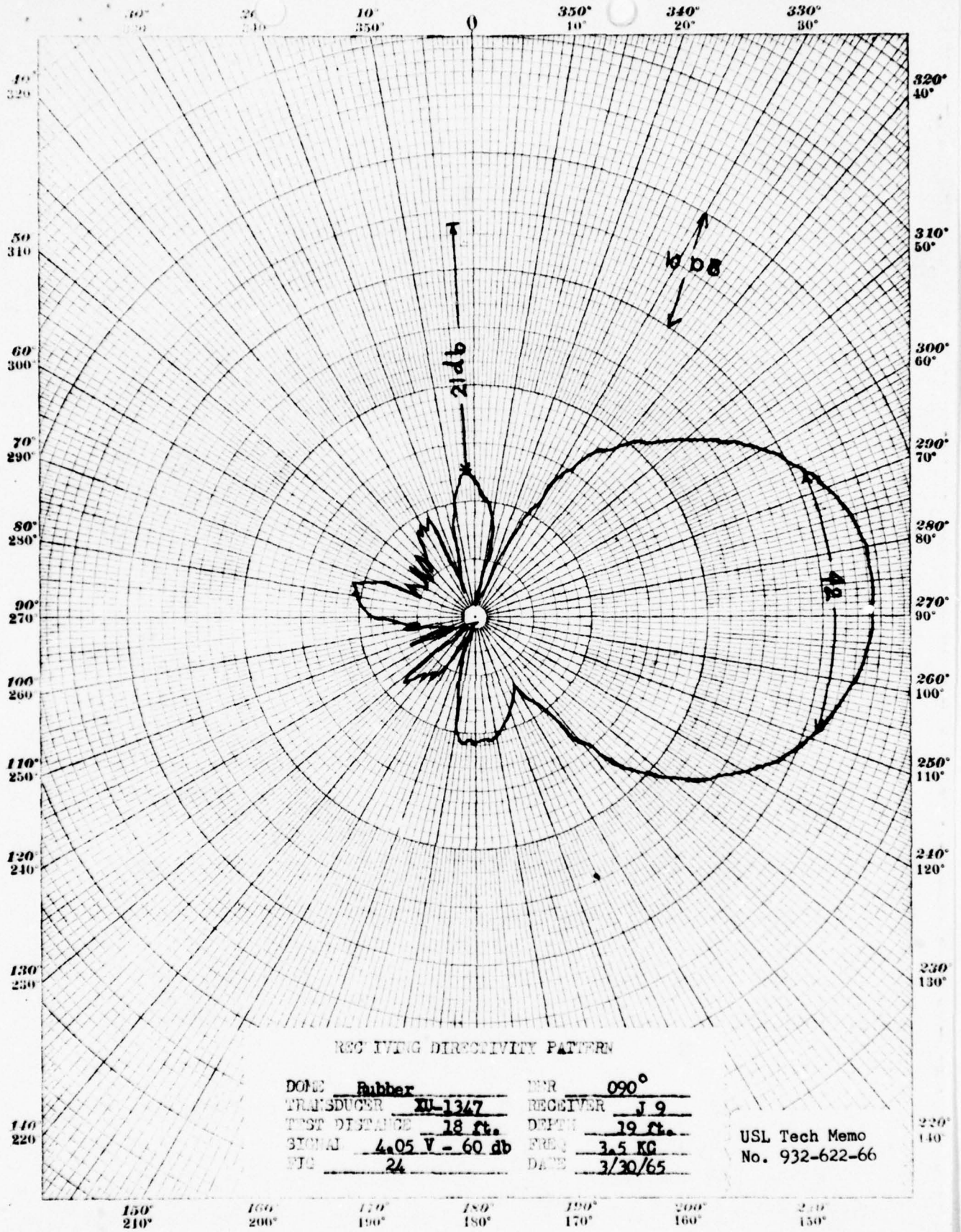

RECEIVING DIRECTIVITY PATTERN

DOME	Rubber	PER	090°
TRANSDUCER	XU-1347	RECEIVER	J 9
TEST DISTANCE	18 ft.	DEPTH	19 ft.
SIGNAL	4.05 V - 60 db	FREQ	3.5 KC
BIG	24	DATE	3/30/65

USL Tech Memo
No. 932-622-66

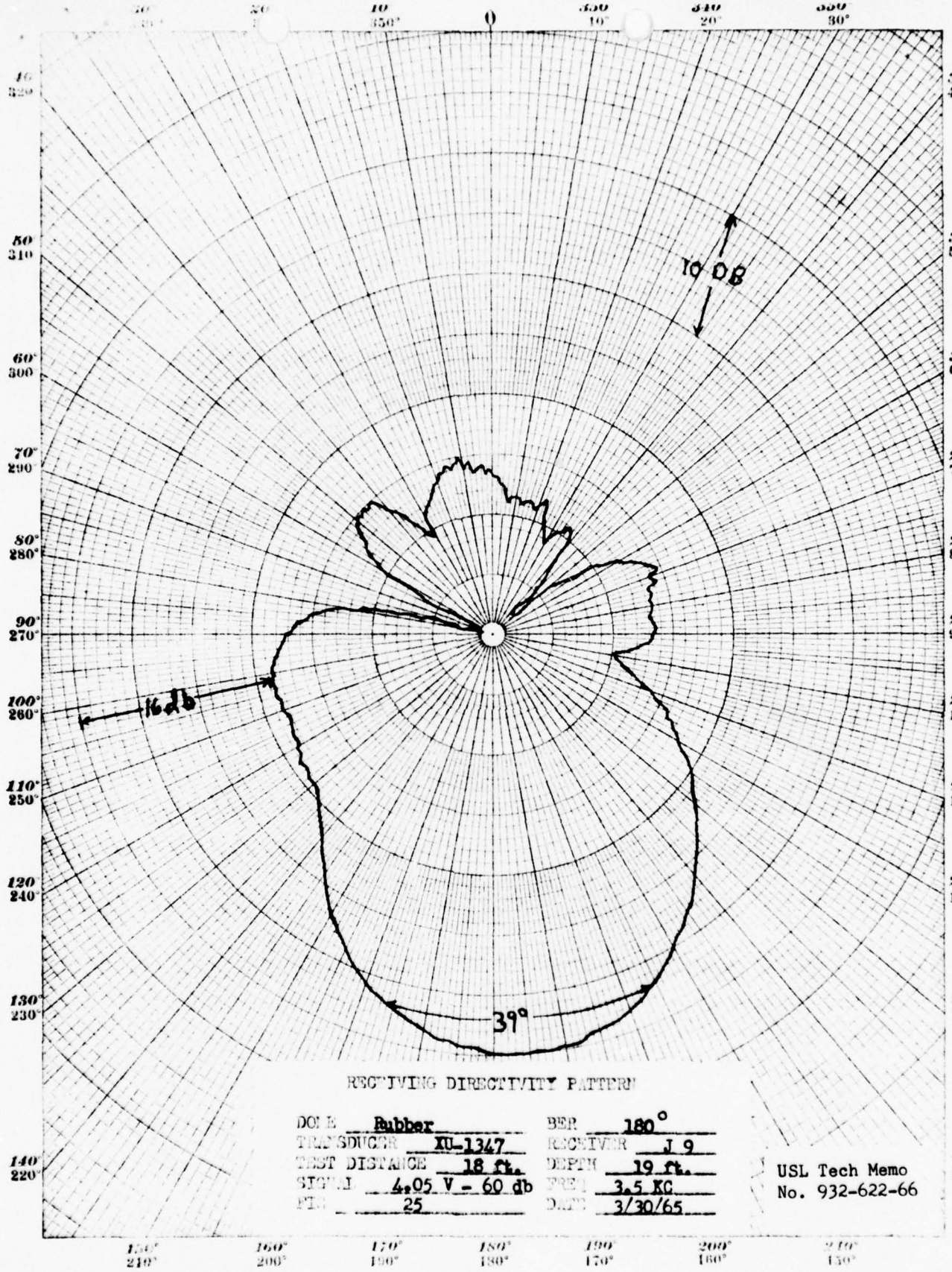

RECEIVING DIRECTIVITY PATTERN

DOME Rubber
TRANSDUCER XU-1347
TEST DISTANCE 18 ft.
SIGNAL 4.05 V - 60 db
FILE 25

NUMBER 180°
RECEIVER J 9
DEPTH 19 ft.
FREQ 3.5 KC
DATE 3/30/65

USL Tech Memo
No. 932-622-66

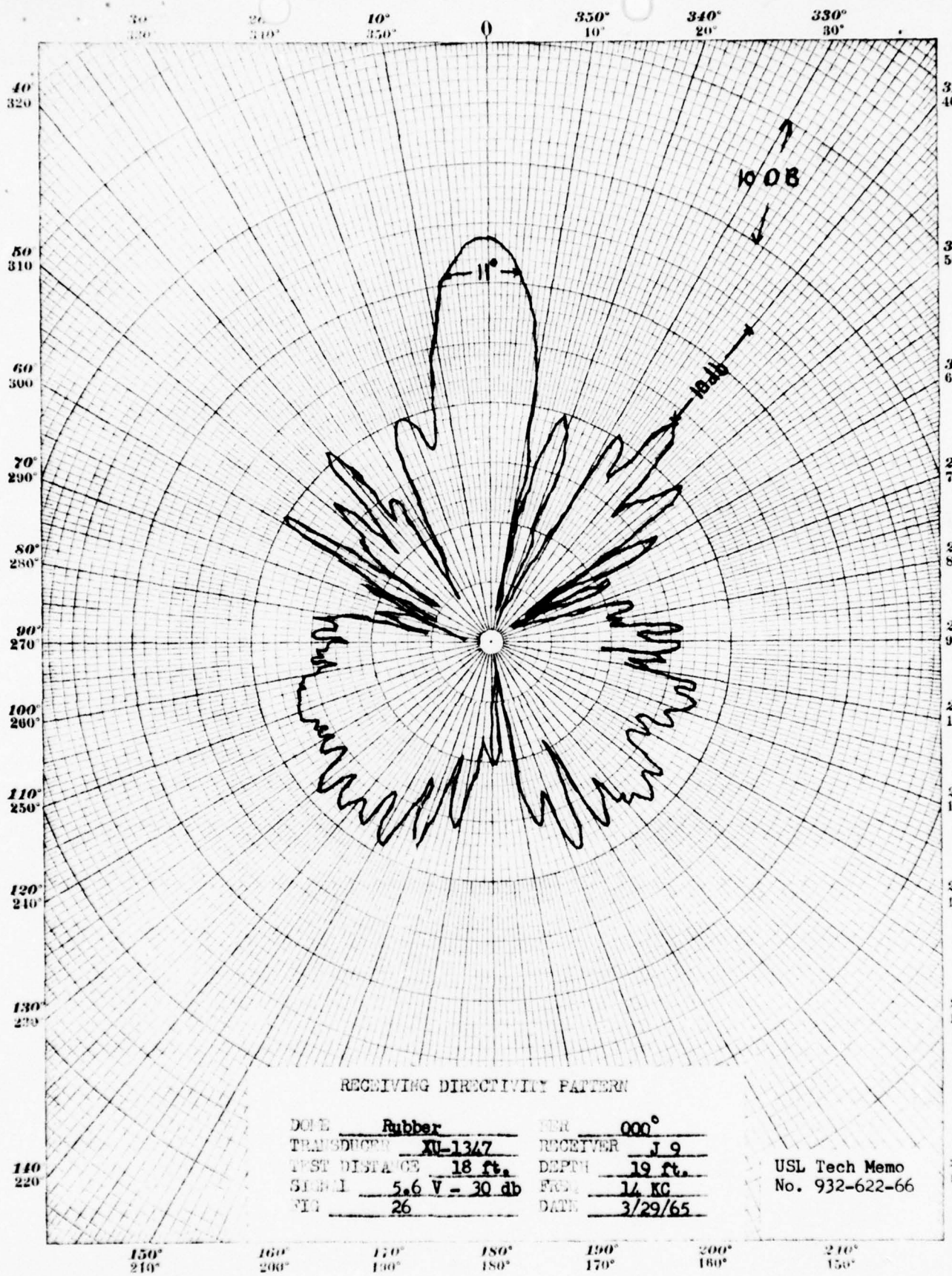

RECEIVING DIRECTIVITY PATTERN

DOME	Rubber	BEAR	000°
TRANSDUCER	XU-1347	RECEIVER	J 9
TEST DISTANCE	18 ft.	DEPTH	19 ft.
SIGNAL	5.6 V - 30 db	FREQ	14 KC
BIT	26	DATE	3/29/65

USL Tech Memo
No. 932-622-66

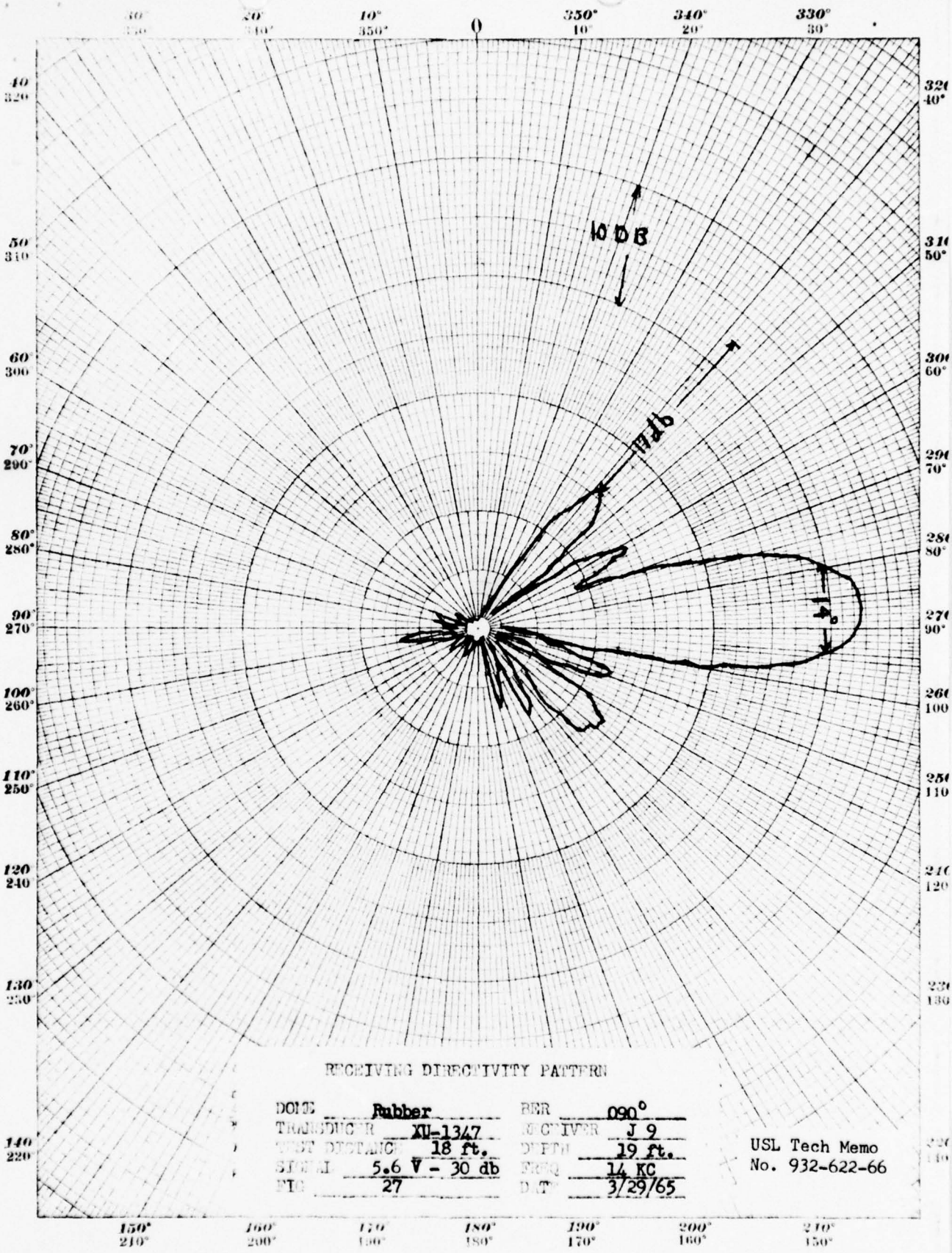

RECEIVING DIRECTIVITY PATTERN

DOCK	Rubber	BEAR	090°
TRANSDUCER	XU-1347	RECEIVER	J 9
[illegible] DISTANCE	18 ft.	DEPTH	19 ft.
SIGNAL	5.6 V - 30 db	FREQ	14 KC
PIC	27	DATE	3/29/65

USL Tech Memo
No. 932-622-66

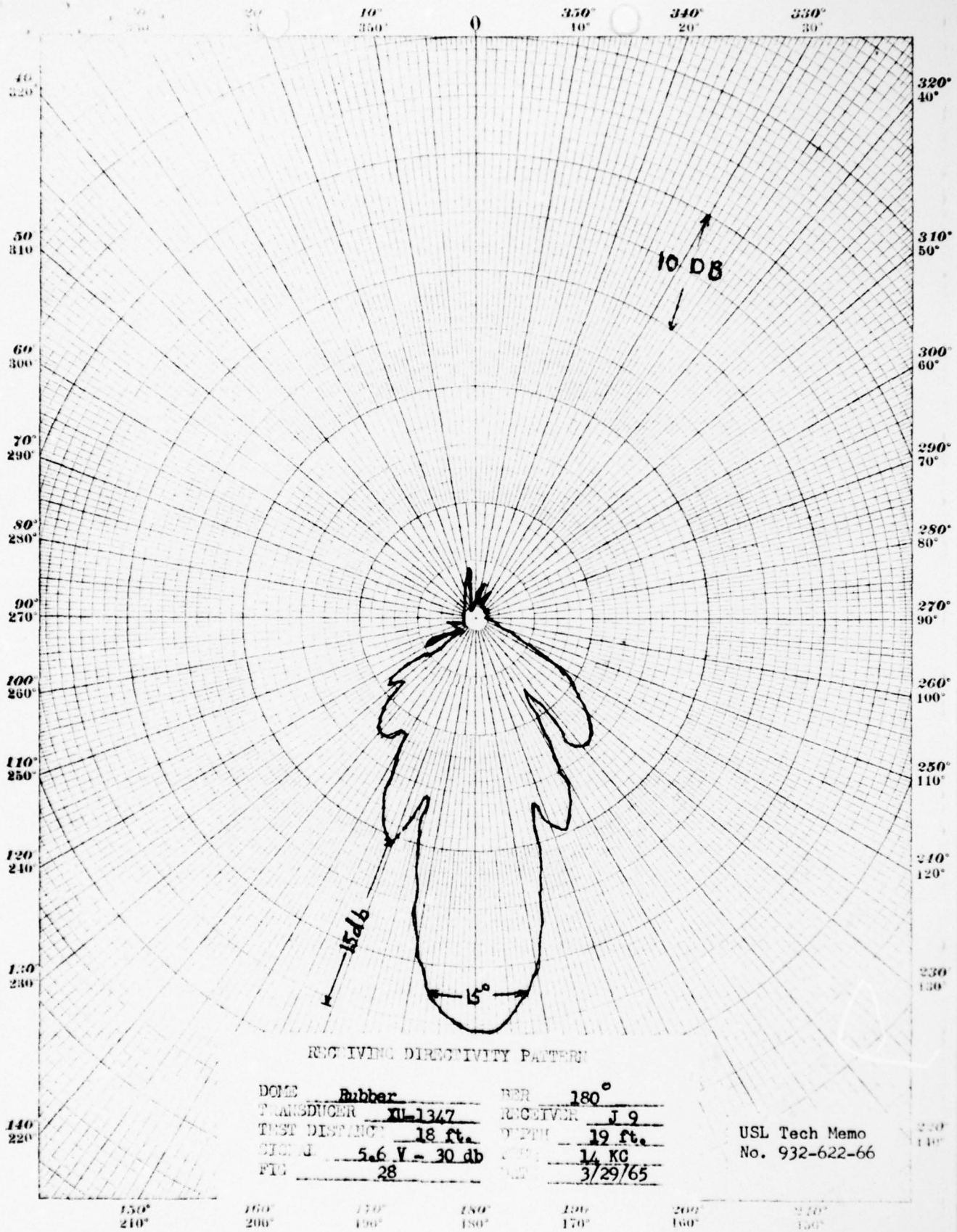

RECEIVING DIRECTIVITY PATTERN

DOME	Rubber	BEAR	180°
TRANSDUCER	XL-1347	RECEIVER	J 9
TEST DISTANCE	18 ft.	DEPTH	19 ft.
SIGNAL	5.6 V - 30 db		14 KC
FILE	28		3/29/65

USL Tech Memo
No. 932-622-66

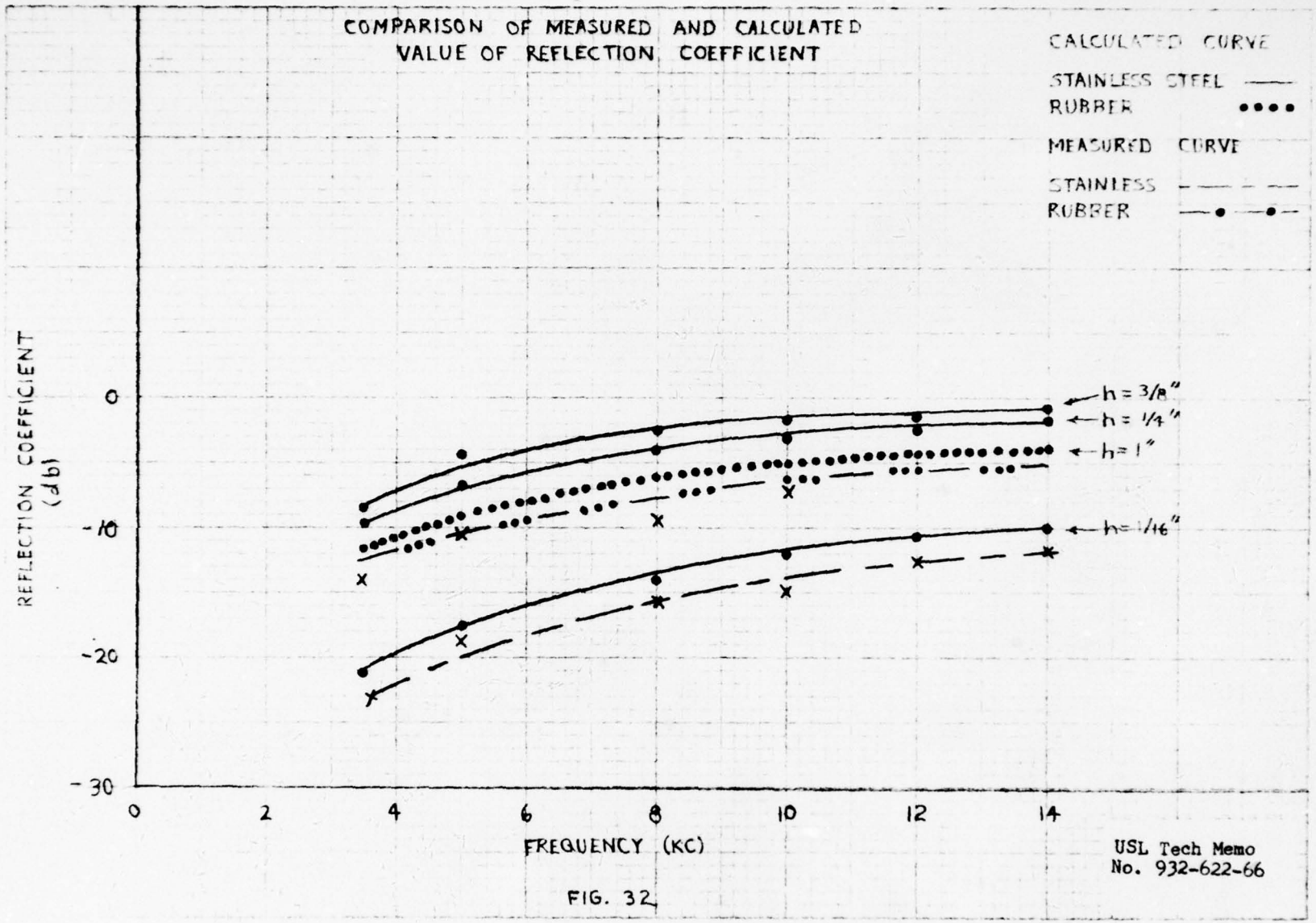
COMPARISON OF MEASURED AND CALCULATED
VALUE OF REFLECTION COEFFICIENT
CALCULATED CURVE
STAINLESS STEEL
RUBBER
MEASURED CURVE
STAINLESS
RUBBER
REFLECTION COEFFICIENT (db)
0
-10
-20
-30
0
2
4
6
8
10
12
14
FREQUENCY (KC)
h = 3/8"
h = 1/4"
h = 1"
h = 1/16"
USL Tech Memo
No. 932-622-66

FIG. 32

FRONT VIEW

REAR VIEW

Fig. 1 - Stainless Steel Dome Section
Skin Thickness = 1/16"

USL Tech Memo No. 932-622-66

U. S. Navy Underwater Sound Laboratory
NP24 - 26548 - 9 - 65

Official Photograph

FRONT VIEW

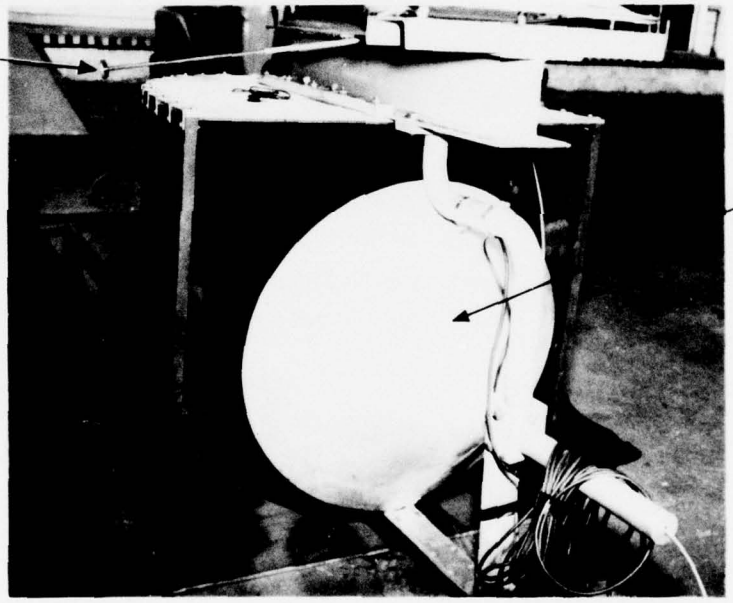

REAR VIEW

Fig. 2 - B. F. Goodrich Rubber Dome Section
Skin Thickness - 1"

USL Tech Memo No. 932-622-66

U. S. Navy Underwater Sound Laboratory
NP24 - 26549 - 9 - 65

Official Photograph

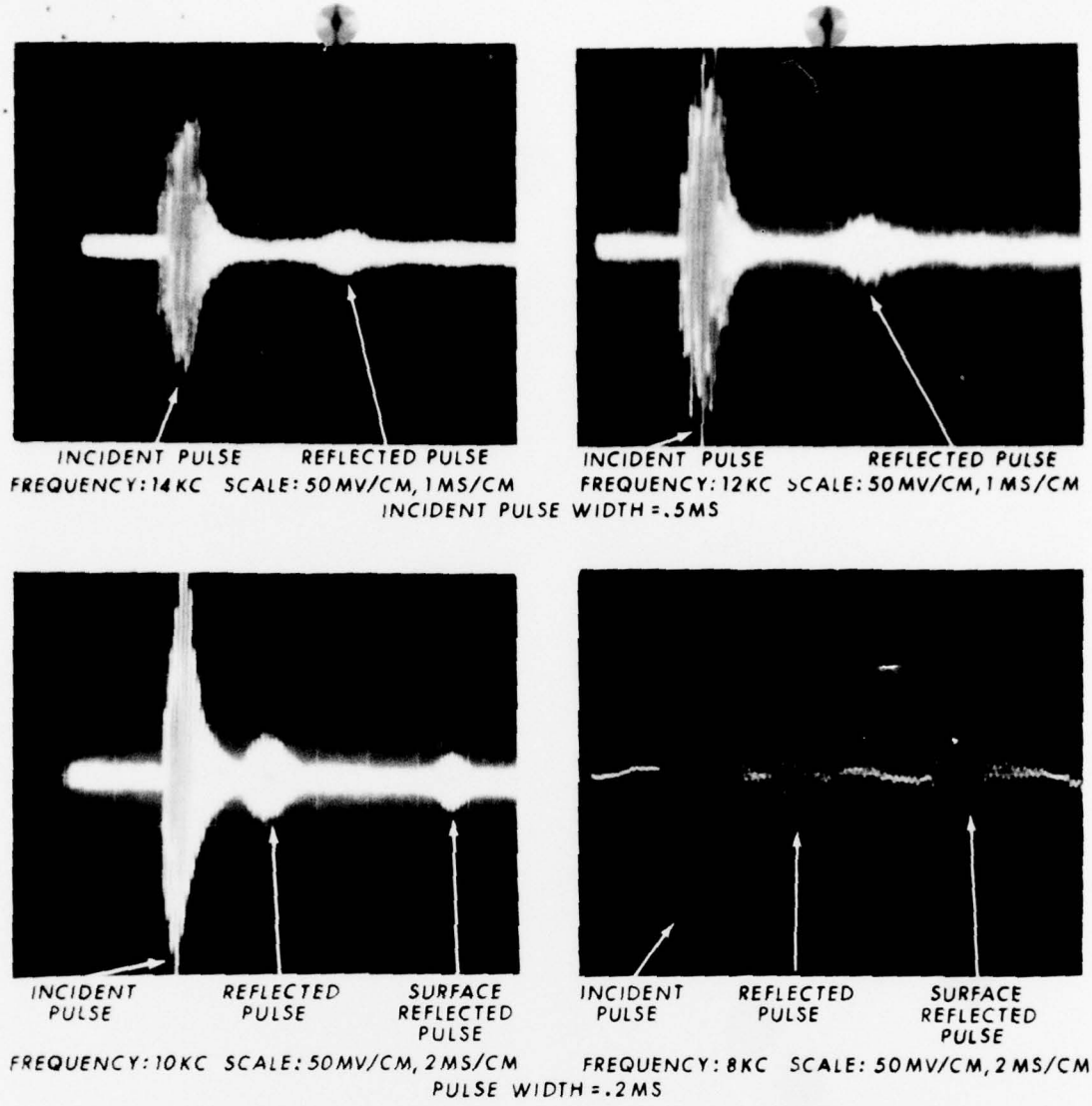

Fig. 30 - Reflection Measurements (090° Bearing)

U. S. Navy Underwater Sound Laboratory
NP24 - 26316 - 7 - 65

Official Photograph

Appendix A

The behavior of a sound wave in a homogeneous medium can be described by a partial differential equation,

$$\nabla^2\psi = \frac{1}{c^2}\frac{\partial^2\psi}{\partial t^2} \tag{1A}$$

commonly called the wave equation. A few of the general properties of this equation are: (1) It is a linear equation, thus it obeys the principle of superposition and, (2) The general solution of this type equation involves arbitrary functions (A_1, A_2 ... etc.). This corresponds physically to the fact that there are an infinite variety of waves. Therefore, to get a solution for a specific type of wave necessitates the introduction of boundary conditions on the wave-bearing medium. The nature of ψ, the acoustic potential, also calls for some comment. It is essentially a mathematical tool by which the combined effects of acoustic pressure and particle velocity, the two main parameters effecting wave motion, can be expressed in a single quantity ψ, where (see reference a)

$$v(\text{Particle Velocity}) = \nabla\psi \tag{2A}$$

$$p(\text{Pressure}) = -\rho\omega\psi \tag{3A}$$

To obtain a general solution to the wave equation, employ the method of separation of variables. In employing this method of solution, assume a solution for ψ in the form of a product of arbitrary functions,

$$\psi = X(x)\,Y(y)\,Z(z)\,T(t) \tag{4A}$$

Now, to find the conditions they must satisfy in order to satisfy the wave equation, substitute the above expression into the wave equation,

$$\frac{\partial^2\psi}{\partial x^2} + \frac{\partial^2\psi}{\partial y^2} + \frac{\partial^2\psi}{\partial z^2} = \frac{1}{c^2}\frac{\partial^2\psi}{\partial t^2} \tag{5A}$$

$$YZT\frac{\partial^2 X}{\partial x^2} + XZT\frac{\partial^2 Y}{\partial y^2} + XYT\frac{\partial^2 Z}{\partial z^2} = \frac{XYZ}{c^2}\frac{\partial^2 T}{\partial t^2} \tag{6A}$$

Dividing both sides of the above equation by XYZT,

$$\frac{1}{X}\frac{\partial^2 X}{\partial x^2} + \frac{1}{Y}\frac{\partial^2 Y}{\partial y^2} + \frac{1}{Z}\frac{\partial^2 Z}{\partial z^2} = \frac{1}{Tc^2}\frac{\partial^2 T}{\partial t^2} \tag{7A}$$

Now, the expression on the right side of the above equation is a function of T, exclusively. The only way it can be identically equal to the left hand side, which is a function of X, Y, and Z, exclusively, is for both sides to be equal to the same constant. For convenience, let this constant be $-K^2$ (the propogation constant or wave number). Thus, the equation for T becomes the second order differential equation,

$$\frac{\partial^2 T}{\partial t^2} + c^2 K^2 T = 0 \tag{8A}$$

which has a solution of the form,

$$T = A_0 e^{jckt} + B_0 e^{-jckt} \tag{9A}$$

It can be seen from the exponent of the exponential, which must have the dimensions of radians, that the product CK must have the dimensions of radians per unit time, which is angular velocity W, therefore $K = W/C$.

Now substituting $-K^2$ into equation (7A), we have,

$$\frac{1}{Y}\frac{\partial^2 Y}{\partial y^2} + \frac{1}{Z}\frac{\partial^2 Z}{\partial z^2} = -k^2 - \frac{1}{X}\frac{\partial^2 X}{\partial x^2} \tag{10A}$$

Using the same technique as previously, it is seen that both sides of the above equation must be equal to the same constant which we will call $-K^2 + k_1^2$ (where k_1 is the component of the wave number in the X direction). This gives us,

$$\frac{\partial^2 X}{\partial x^2} + k_1^2 X = 0 \tag{11A}$$

Similarly, we introduce two other constants k_2^2 and k_3^2 which give,

$$\frac{\partial^2 Y}{\partial y^2} + k_2^2 Y = 0 \tag{12A}$$

$$\frac{\partial^2 Z}{\partial z^2} + k_3^2 Z = 0 \tag{13A}$$

where, $K^2 = k_1^2 + k_2^2 + k_3^2$ (14A)

The solutions of the second order linear equations for X, Y, and Z are,

$$X = A_1 e^{-jk_1 x} + B_1 e^{jk_1 x} \tag{15A}$$

$$Y = A_2 e^{-ik_2 y} + B_2 e^{ik_2 y} \tag{16A}$$

$$Z = A_3 e^{-ik_3 z} + B_3 e^{ik_3 z} \tag{17A}$$

where the A;s and B's are arbitrary constants. The complete solution to the wave equation is,

$$\psi = (A_1 e^{-ik_1 x} + B_1 e^{ik_1 x})(A_2 e^{-ik_2 y} + B_2 e^{ik_2 y})(A_3 e^{-ik_3 z} + B_3 e^{ik_3 z})(A_4 e^{-ickt} + B_4 e^{-ickt}) \tag{18A}$$

As can be observed from the above expression, the possible number of solutions to the wave equation is very large (remembering superposition). But in our case, we are interested in a plane harmonic progressive wave which is one of the above cases. Therefore, arbitrarily set B0, B1, B2 and B3 equal to zero, and assume that

$k_1 \equiv k\alpha$, $k_2 \equiv k\beta$, and $k_3 \equiv k\Gamma$

where α, β, and Γ are direction cosines and $\alpha^2 + \beta^2 + \Gamma^2 = 1$
Thus our solution takes the desired form,

$$\psi = A e^{-i[wt - k(\alpha x + \beta y + \Gamma z)]} \tag{19A}$$

From the solution of the wave equation, we know the general form of the expressions for the incident and transmitted waves on a flat surface. Let us now take the case of the stainless steel dome skin which is essentially a three-layer problem (see Figure A below).

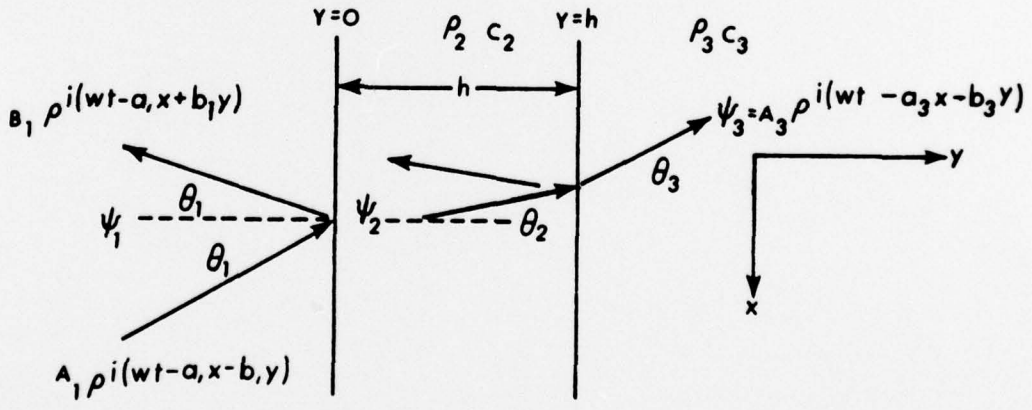

FIG. A

The solutions to the wave equation for the general case of oblique incidence are,

$$\psi_1 = A_1 e^{i(\omega t - a x - b_1 y)} + B_1 e^{i(\omega t - a x + b_1 y)} \quad (20A)$$

$$\psi_2 = A_2 e^{i(\omega t - a x - b_2 y)} + B_2 e^{i(\omega t - a x + b_2 y)} \quad (21A)$$

$$\psi_3 = A_3 e^{i(\omega t - a x - b_3 y)} \quad (22A)$$

from the above figure, the quantities b_1, b_2, b_3, and a are defined as,

$$b_1 \equiv k_1 \cos\theta \equiv \frac{2\pi f}{c_1}\cos\theta_1 \qquad b_2 \equiv \frac{2\pi f}{c_2}\cos\theta_2 \qquad b_3 \equiv \frac{2\pi f}{c_3}\cos\theta_3$$

$$a \equiv k_1 \sin\theta_1 \equiv \frac{2\pi f}{c_1}\sin\theta_1 \equiv \frac{2\pi f}{c_2}\sin\theta_2 \equiv \frac{2\pi f}{c_3}\sin\theta_3$$

LET $S_1 \equiv \frac{c_1}{\cos\theta_1}$ $S_2 \equiv \frac{c_2}{\cos\theta_2}$ $S_3 = \frac{c_3}{\cos\theta_3}$

$$b_1 \equiv \frac{2\pi f}{S_1} \qquad b_2 \equiv \frac{2\pi f}{S_2} \qquad b_3 \equiv \frac{2\pi f}{S_3}$$

Now, applying the boundary conditions (See reference (1)):

1. the pressure must be continuous across the boundary.
2. the vertical component of velocity must be continuous across the boundary.

$$\rho_1 \frac{\partial \psi_1}{\partial t} = \rho_2 \frac{\partial \psi_2}{\partial t} \quad (23A) \qquad \rho_2 \frac{\partial \psi_2}{\partial t} = \rho_3 \frac{\partial \psi_3}{\partial t} \quad (24A) \quad (23A)$$

at $y = 0$ (24A)

$$\frac{\partial \psi_1}{\partial y} = \frac{\partial \psi_2}{\partial y} \qquad \text{at } y = h \qquad \frac{\partial \psi_2}{\partial y} = \frac{\partial \psi_3}{\partial y}$$

Substituting the expressions for ψ_1, ψ_2, and ψ_3 into the boundary conditions, we have,

$$\rho_1 A_1 + \rho_1 B_1 = \rho_2 A_2 + \rho_2 B_2$$

$$S_2 A_1 - S_2 B_1 = S_1 A_2 - S_1 B_2$$

$$\rho_2 e^{-ib_2 h} A_2 + \rho_2 e^{ib_2 h} B_2 = \rho_3 e^{-ib_3 h} A_3$$

$$S_3 e^{-ib_2 h} A_2 - S_3 e^{ib_2 h} B_2 = S_2 e^{-ib_3 h} A_3$$

Rearanging the above equations in determinant form,

$$-\rho_1 B_1 + \rho_2 A_2 + \rho_2 B_2 + 0 = \rho_1 A_1 \tag{25A}$$

$$s_2 B_1 + s_1 A_2 - s_1 B_2 + 0 = s_2 A_1 \tag{26A}$$

$$0 + \rho_2 e^{-ib_2 h} A_2 + \rho_2 e^{ib_2 h} B_2 - \rho_3 e^{-ib_3 h} A_3 = 0 \tag{27A}$$

$$0 + s_3 e^{-ib_2 h} A_2 + s_3 e^{ib_2 h} B_2 - s_2 e^{-ib_3 h} A_3 = 0 \tag{28A}$$

Now, solving for the reflection coefficient.

$$R = \frac{B_1}{A_1} = \frac{\begin{vmatrix} \rho_1 & \rho_2 & \rho_2 & 0 \\ s_2 & s_1 & -s_1 & 0 \\ 0 & \rho_2 e^{-ib_2 h} & \rho_2 e^{ib_2 h} & -\rho_3 e^{-ib_3 h} \\ 0 & s_3 e^{-ib_2 h} & -s_3 e^{ib_2 h} & -s_2 e^{-ib_3 h} \end{vmatrix}}{\begin{vmatrix} -\rho_1 & \rho_2 & \rho_2 & 0 \\ s_2 & s_1 & -s_1 & 0 \\ 0 & \rho_2 e^{-ib_2 h} & \rho_2 e^{ib_2 h} & -\rho_3 e^{-ib_3 h} \\ 0 & s_3 e^{-ib_2 h} & -s_3 e^{ib_2 h} & -s_2 e^{-ib_3 h} \end{vmatrix}} \tag{29A}$$

Where the solution to the above determinant is:

$$R = \frac{B_1}{A_1} = \frac{(\rho_1 s_1 - \rho_2 s_2)(-\rho_2 s_2 - \rho_3 s_3) e^{ib_2 h} + (\rho_1 s_1 + \rho_2 s_2)(-\rho_2 s_2 + \rho_3 s_3) e^{-ib_2 h}}{(\rho_1 s_1 - \rho_2 s_2)(-\rho_2 s_2 - \rho_3 s_3) e^{ib_2 h} + (-\rho_1 s_1 + \rho_2 s_2)(-\rho_2 s_2 + \rho_3 s_3) e^{-ib_2 h}} \tag{30A}$$

The above expression is general for any three-layer problem. If the velocity (c), the density (e), the thickness of the center layer (h), and the angle of initial incidence are known, the reflection coefficient can be calculated for any frequency.

Now, expressing equation 30A in terms of sines and cosines by means of the following identities, $e^{-1x} = \cos x - 1 \sin x$ and $e^{1x} = \cos x + 1 \sin x$, and simplifying, we have,

$$R = \frac{B_1}{A_1} = \frac{(-1 + m_1 m_2)\cos(b_2 h) + 1(m_1 - m_2)\sin(b_2 h)}{(1 + m_1 m_2)\cos(b_2 h) + 1(m_1 + m_2)\sin(b_2 h)} \tag{31A}$$

where

$$m_1 \equiv \rho_2 S_2 / \rho_1 S_1 \qquad m_2 \equiv \rho_3 S_3 / \rho_2 S_2$$

In our particular case, medium 1 and medium 3 are identical (water), therefore, $\rho_1 = \rho_3$ $c_1 = c_3$ $\therefore m_1 = 1/m_2$ Under these conditions, the reflection coefficient becomes,

$$R = \frac{1\left(\frac{\rho_2 S_2}{\rho_1 S_1} - \frac{\rho_1 S_1}{\rho_2 S_2}\right)\sin(b_2 h)}{2\cos(b_2 h) + 1\left(\frac{\rho_2 S_2}{\rho_1 S_1} + \frac{\rho_1 S_1}{\rho_2 S_2}\right)\sin(b_2 h)} \tag{32A}$$

$$|R| = \frac{\left(\frac{\rho_2 S_2}{\rho_1 S_1} - \frac{\rho_1 S_1}{\rho_2 S_2}\right)^2 \sin^2\left(\frac{2\pi f h}{s_2}\right)}{4\cos^2\left(\frac{2\pi f h}{s_2}\right) + \left(\frac{\rho_2 S_2}{\rho_1 S_1} + \frac{\rho_1 S_1}{\rho_2 S_2}\right)\sin^2\left(\frac{2\pi f h}{s_2}\right)} e^{1\phi} \tag{33A}$$

$$\phi = 90^\circ - \tan^{-1}\left[\frac{1}{2}\left(\frac{\rho_2 S_2}{\rho_1 S_1} + \frac{\rho_1 S_1}{\rho_2 S_2}\right)\sin\left(\frac{2\pi f h}{s_2}\right)\right] \tag{34A}$$

For the stainless steel dome (assuming normal incidence, which was the condition in the actual tests) we have,

$$m_1 = \frac{\rho_2 c_2}{\rho_1 c_1} = \frac{7.7\ \text{gm/cm}^3 \cdot 5.2\times10^5\ \text{cm/sec}}{1\ \text{gm/cm}^3 \cdot 1.5\times10^5\ \text{cm/sec}} = 26.7$$

$$m_2 = \frac{1}{m_1} = .0375 \qquad h = 1/16'' = .159\ \text{cm}$$

$$\frac{2\pi f h}{c_2} = .18\times10^{-5} f$$

$$|R| = \frac{713 \sin^2(.18\times10^{-5} f)}{4\cos^2(.18\times10^{-5} f) + 713 \sin^2(.18\times10^{-5} f)} \tag{35A}$$

$$\phi = 90^\circ - \tan^{-1}\left[13.4 \sin(.18\times10^{-5} f)\right] \tag{36A}$$

For $f = 3.55$ KC $\quad |R| = .059$ and $\phi = 85^\circ$

See Table IV for the results with other frequencies, angles of incidence, and thicknesses.

Appendix B

Now, we will consider the reflection coefficient from the rubber dome. The material which makes up the dome has three distinct layers (see Figure B, below).

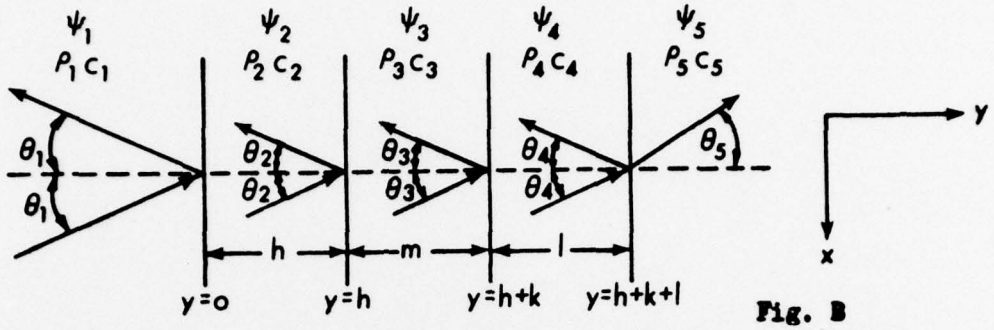

Fig. B

Characterize the sound field by the acoustic potential ψ. The particle velocity and acoustic pressure in the sound wave will be expressed through ψ by,

$$v(\text{Particle Velocity}) = -\nabla\psi \tag{1B}$$

$$p(\text{Sound Pressure}) = -i\omega\rho\psi \tag{2B}$$

The acoustic potential, ψ, is a derived term which is used as a mathematical tool. The assumed solutions to the wave equation in the different layers are:

$$\psi_1 = A_1 e^{i(\omega t - a_1 x - b_1 y)} + B_1 e^{i(\omega t - a_1 x + b_1 y)} \tag{3B}$$

$$\psi_2 = A_2 e^{i(\omega t - a_2 x - b_2 y)} + B_2 e^{i(\omega t - a_2 x + b_2 y)} \tag{4B}$$

$$\psi_3 = A_3 e^{i(\omega t - a_3 x - b_3 y)} + B_3 e^{i(\omega t - a_3 x + b_3 y)} \tag{5B}$$

$$\psi_4 = A_4 e^{i(\omega t - a_4 x - b_4 y)} + B_4 e^{i(\omega t - a_4 x + b_4 y)} \tag{6B}$$

$$\psi_5 = A_5 e^{i(\omega t - a_5 x - b_5 y)} \tag{7B}$$

where

$$b_1 = k_1 \cos\theta_1 = \frac{2\pi f}{c_1}\cos\theta_1 \qquad b_2 = \frac{2\pi f}{c_2}\cos\theta_2$$

$$b_3 = \frac{2\pi f}{c_3}\cos\theta_3 \qquad b_4 = \frac{2\pi f}{c_4}\cos\theta_4 \qquad b_5 = \frac{2\pi f}{c_5}\cos\theta_5$$

$$a_1 = k_1 \sin\theta_1 = \frac{2\pi f}{c_1}\sin\theta_1 = a_2 = a_3 = a_4 = a_5 \quad \text{(SNELL'S LAW)}$$

LET

$$S_1 = \frac{c_1}{\cos\theta_1} \qquad S_2 = \frac{c_2}{\cos\theta_2} \qquad S_3 = \frac{c_3}{\cos\theta_3} \qquad S_4 = \frac{c_4}{\cos\theta_4} \qquad S_5 = \frac{c_5}{\cos\theta_5}$$

$$\therefore\ b_1 = \frac{2\pi f}{S_1} \quad b_2 = \frac{2\pi f}{S_2} \quad b_3 = \frac{2\pi f}{S_3} \quad b_4 = \frac{2\pi f}{S_4} \quad b_5 = \frac{2\pi f}{S_5}$$

The boundary conditions which hold for this case are the continuity of pressure and the vertical component of particle velocity across each boundary,

$$\text{AT } y = 0 \qquad \rho_1 \frac{\partial \psi_1}{\partial t} = \rho_2 \frac{\partial \psi_2}{\partial t} \qquad \frac{\partial \psi_1}{\partial y} = \frac{\partial \psi_2}{\partial y} \tag{8B}$$

$$\rho_2 \frac{\partial \psi_2}{\partial x} = \rho_3 \frac{\partial \psi_3}{\partial x}$$

AT $y = h$ (9B)

$$\frac{\partial \psi_2}{\partial y} = \frac{\partial \psi_3}{\partial y}$$

$$\rho_3 \frac{\partial \psi_3}{\partial x} = \rho_4 \frac{\partial \psi_4}{\partial x}$$

AT $y = h + M = E$ (10B)

$$\frac{\partial \psi_3}{\partial y} = \frac{\partial \psi_4}{\partial y}$$

$$\rho_4 \frac{\partial \psi_4}{\partial x} = \rho_5 \frac{\partial \psi_5}{\partial x}$$

AT $y = h + M + l = P$ (11B)

$$\frac{\partial \psi_4}{\partial y} = \frac{\partial \psi_5}{\partial y}$$

Applying the boundary conditions, we have,

$$\rho_1 [A_1 + B_1] = \rho_2 [A_2 + B_2] \quad \text{(12B)}$$

AT $y = 0$

$$S_2 [A_1 - B_1] = S_1 [A_2 - B_2] \quad \text{(13B)}$$

$$\rho_2\left[A_2 e^{-ib_2 h} + B_2 e^{ib_2 h}\right] = \rho_3\left[A_3 e^{-ib_3 h} + B_3 e^{ib_3 h}\right] \tag{14B}$$

At $y = h$

$$S_3\left[A_2 e^{-ib_2 h} - B_2 e^{ib_2 h}\right] = S_2\left[A_3 e^{-ib_3 h} - B_3 e^{ib_3 h}\right] \tag{15B}$$

$$\rho_3\left[A_3 e^{-ib_3 E} + B_3 e^{ib_3 E}\right] = \rho_4\left[A_4 e^{-ib_4 E} + B_4 e^{ib_4 E}\right] \tag{16B}$$

At $y = h + M = E$

$$S_4\left[A_3 e^{-ib_3 E} - B_3 e^{ib_3 E}\right] = S_3\left[A_4 e^{-ib_4 E} - B_4 e^{ib_4 E}\right] \tag{17B}$$

$$\rho_4\left[A_4 e^{-ib_4 P} + B_4 e^{ib_4 P}\right] = \rho_5 A_5 e^{-ib_5 P} \tag{18B}$$

At $y = h + M + \ell = P$

$$S_5\left[A_4 e^{-ib_4 P} - B_4 e^{ib_4 P}\right] = S_4 A_5 e^{-ib_5 P} \tag{19B}$$

Now, putting the above equation in determinant form, and solving for the reflection coefficient,

$$R = \frac{B_1}{A_1} = \frac{\begin{vmatrix} \rho_1 & \rho_2 & \rho_2 & 0 & 0 & 0 & 0 & 0 \\ S_2 & S_1 & -S_1 & 0 & 0 & 0 & 0 & 0 \\ 0 & \rho_2 e^{-ib_2 h} & \rho_2 e^{ib_2 h} & -\rho_3 e^{-ib_3 h} & -\rho_3 e^{ib_3 h} & 0 & 0 & 0 \\ 0 & S_2 e^{-ib_2 h} & -S_2 e^{ib_2 h} & -S_3 e^{-ib_3 h} & S_3 e^{ib_3 h} & 0 & 0 & 0 \\ 0 & 0 & 0 & \rho_3 e^{-ib_3 E} & \rho_3 e^{ib_3 E} & -\rho_4 e^{-ib_4 E} & -\rho_4 e^{ib_4 E} & 0 \\ 0 & 0 & 0 & S_3 e^{-ib_3 E} & -S_3 e^{ib_3 E} & -S_4 e^{-ib_4 E} & S_4 e^{ib_4 E} & 0 \\ 0 & 0 & 0 & 0 & 0 & \rho_4 e^{-ib_4 P} & \rho_4 e^{ib_4 P} & \rho_5 e^{-ib_5 P} \\ 0 & 0 & 0 & 0 & 0 & S_4 e^{-ib_4 P} & -S_4 e^{ib_4 P} & -S_5 e^{-ib_5 P} \end{vmatrix}}{\begin{vmatrix} -\rho_1 & \rho_2 & \rho_2 & 0 & 0 & 0 & 0 & 0 \\ S_2 & S_1 & -S_1 & 0 & 0 & 0 & 0 & 0 \\ 0 & \rho_2 e^{-ib_2 h} & \rho_2 e^{ib_2 h} & -\rho_3 e^{-ib_3 h} & -\rho_3 e^{ib_3 h} & 0 & 0 & 0 \\ 0 & S_2 e^{-ib_2 h} & -S_2 e^{ib_2 h} & -S_3 e^{-ib_3 h} & S_3 e^{ib_3 h} & 0 & 0 & 0 \\ 0 & 0 & 0 & \rho_3 e^{-ib_3 E} & \rho_3 e^{ib_3 E} & -\rho_4 e^{-ib_4 E} & -\rho_4 e^{ib_4 E} & 0 \\ 0 & 0 & 0 & S_3 e^{-ib_3 E} & -S_3 e^{ib_3 E} & -S_4 e^{-ib_4 E} & S_4 e^{ib_4 E} & 0 \\ 0 & 0 & 0 & 0 & 0 & \rho_4 e^{-ib_4 P} & \rho_4 e^{ib_4 P} & \rho_5 e^{-ib_5 P} \\ 0 & 0 & 0 & 0 & 0 & S_5 e^{-ib_4 P} & -S_5 e^{ib_4 P} & -S_4 e^{-ib_5 P} \end{vmatrix}} \qquad (20B)$$

The above matrix, which would be very tedious to solve longhand, was programmed on the computer. The parameters which are needed by the computer for this computation are ρ, c and the thickness of each layer, along with the initial angle of incidence. The results of this computation for the desired frequencies are shown in Table IV.